

**MASTER'S DEGREE IN
SPACE SCIENCE AND TECHNOLOGY**

MASTER'S THESIS

***THERMAL DIFFUSIVITY MEASUREMENTS BY
FLYING-SPOT INFRARED THERMOGRAPHY***

Estudiante *Ordóñez, Devesa, Jon*
Director/Directora *Mendioroz, Astigarraga, Maria Aranzazu*
Departamento
Curso académico *2021/2022*

Bilbao, September 2022

RESUMEN

En este trabajo de fin de máster se desarrolla un método experimental para medir la difusividad y, en un futuro, detectar grietas con un haz móvil, que puede escanear la superficie de la muestra y sondear diferentes regiones, con el objetivo de obtener resultados experimentales de medidas de difusividad en diferentes materiales. Para ello, se ha utilizado el método flying spot, que es un ensayo no destructivo. Para entender cómo se ha llevado a cabo el experimento, se habla primero de la termografía en general y luego se centra en el método del flying spot. Después, hay una sección teórica específica de este método para demostrar de dónde proceden las ecuaciones utilizadas para calcular el valor de la difusividad térmica. También se describe el equipo utilizado, así como su funcionamiento y limitaciones. A continuación, se presentan y discuten los resultados obtenidos y el trabajo concluye con un resumen y trabajos futuros en este sentido.

ABSTRACT

In this master's thesis an experimental method is developed to measure diffusivity and, in the future, detect cracks with a moving laser spot, which can scan the surface of the sample and probe different regions, with the aim of obtaining experimental results of diffusivity measurements in different materials. For this purpose, the flying spot method, which is a non-destructive test, has been used. To understand how the experiment was carried out, thermography in general is first discussed and then focus on the flying spot method. After that, there is a theoretical section specific to this method to demonstrate where the equations used to calculate the diffusivity value come from. There is also a description of the equipment used, as well as its operation and limitations. Then, the results obtained are presented and discussed and the work concludes with a summary and future work in this.

LABURPENA

Master-amaierako lan honetan, difusibitatea neurtzeko eta, etorkizunean, laser-puntu mugikor batekin pitzadurak detektatzeko metodo experimental bat garatzen da. Pitzadura horiek laginaren azalera eskaneatu eta zenbait eskualde zundatu ditzakete, hainbat materialetako difusibitate-neurrien emaitza esperimentalak lortzeko. Horretarako, flying spot metodoa erabili da, saiakuntza ez-suntsitzaila. Esperimentua nola egin den ulertzeko, lehenbizi termografiar hitz egiten da, oro har, eta, gero, flying spotaren metodoa aztertzen da. Ondoren, metodo horren atal teoriko espezifikoa bat dago, difusibitatearen balioa kalkulatzeko erabilitako ekuazioak nondik datozen frogatzeko. Erabilitako ekipoa, funtzionamendua eta mugak ere deskribatzen dira. Ondoren, lortutako emaitzak aurkeztu eta eztabaidatu dira, eta lana amaitzeko, laburpen bat egin da, eta etorkizuneko lanak egin dira.

Index

1. Introduction.....	6
2. Theory of flying spot thermography: laser in motion at constant speed	11
3. Experimental device.....	15
3.1 Setup.....	15
3.2 How to perform a measurement.....	17
4. Results of the experimental measurements.....	20
4.1 Analysis procedure.....	20
4.2 Measurement results.....	24
<i>4.2.1 AISI-304, 5.17 mm/s at 1 W</i>	<i>24</i>
<i>4.2.2 PEEK, 0.91 mm/s at 0.01 W.....</i>	<i>26</i>
<i>4.2.3 Glass, 3.78 mm/s at 0.01 W.....</i>	<i>28</i>
5. Conclusions and future work.....	31
References.....	32
Appendix I.....	34
Appendix II.....	44
Appendix III.....	45
Appendix IV	46
Appendix V.....	48

Figure Index

Figure 1 Aspects to be considered in a thermography inspection.....	7
Figure 2 Relevant aspects to the flying spot thermography	9
Figure 3 Schematic of the problem.....	11
Figure 4 Representation of the calculated temperature distribution in steady-state for AISI-304. (a) Surface temperature and (b) $x=0$ section [11].....	12
Figure 5 Representation of the natural logarithm of the temperature times the distance to the laser spot. (a) longitudinal profile, (b) transverse profile and (c) depth profile [12].....	14
Figure 6 The longitudinal profile at different times. (a) difference in the graph when switching the time at which the laser is turned on and (b) minimum time to reach the steady state for different diffusivity values [12].....	14
Figure 7 Scheme of the experimental setup	15
Figure 8 The galvanometric mirrors and the F-Theta lens [13]	16
Figure 9 a) spherical lens, b) Flat-Field scanning lens and c) F-Theta lens.....	16
Figure 10 Flying spot software interface	18
Figure 11 Graphs of the natural logarithm of the temperature times the distance to the laser spot for the longitudinal and transverse profiles of a single laser spot position for AISI-304 at 1 W	22
Figure 12 Graphs of the natural logarithm of the temperature times the distance to the laser spot for the average of the longitudinal profile of four consecutive laser spot positions and transverse profile for the whole length	23
Figure 13 Thermogram corresponding to AISI-304, 5,17 mm/s at 1 W	24
Figure 14 Averaged longitudinal profiles from frames 294 to 306 of AISI-304, 5,17 mm/s at 1 W	25
Figure 15 Averaged transverse profiles from frames 178 to 358 of AISI-304, 5,17 mm/s at 1 W	25
Figure 16 Thermogram corresponding to PEEK, 0,91 mm/s at 0,01 W	26
Figure 17 Averaged longitudinal profiles from frames 1600 to 1612 of PEEK, 0,91 mm/s at 0,01 W	27
Figure 18 Averaged transverse profiles from frames 860 to 1760 of PEEK, 0,91 mm/s at 0,01 W	27
Figure 19 Thermogram corresponding to glass, 3,78 mm/s at 0,01 W	28
Figure 20 Averaged longitudinal profiles from frames 400 to 412 of glass, 3,78 mm/s at 0,01 W	29
Figure 21 Averaged transverse profiles from frames 220 to 440 of glass, 3,78 mm/s at 0,01 W	29
Figure 22 Sequence of temperature profiles along the x axis for an AISI-304 sample with an infinite vertical crack at plane $x = 0$	31
Figure 24 Flying spot software interface	34
Figure 25 Pulse grid flying spot example	36
Figure 26 Vertical line example.....	37
Figure 27 Horizontal line example	37
Figure 28 Single line angle at 45° example.....	38
Figure 29 Single line angle at -45° example	38
Figure 30 Single line angle at 90° example.....	39
Figure 31 Single line angle at -90° example	39
Figure 32 Measurement preparation 1	41
Figure 33 Measurement preparation 2	41
Figure 34 Measurement preparation 3	42
Figure 35 Measurement preparation 4	43

Table Index

Table 1 Intended velocities for the laser spot and the corresponding parameters for the flying spot software.....	21
Table 2 Velocities and parameter to be entered in the flying spot software	22
Table 3 Flying spot software parameters for AISI-304, 5,17 m/s.....	24
Table 4 Flying spot software parameters for PEEK, 0.91 mm/s.....	26
Table 5 Flying spot software parameters for glass, 3.78 mm/s.....	28
Table 6 Diffusivity results for AISI-304 at different velocities	30
Table 7 Diffusivity results for PEEK at different velocities	30
Table 8 Diffusivity results for glass at different velocities	30

1. Introduction

In this work thermography, which will be defined later on, is used to measure the thermal diffusivity of certain materials. Diffusivity is a thermal property of materials that describes how the material behave in a transient situation, when the heat fluxes are not constant. More specifically, it measures the rate at which the heat transfers in a material, from the hot end to the cold one. Diffusivity is denoted by different letters but in this work the letter D will be used. Looking at the formula it can be seen that the thermal diffusivity is the thermal conductivity k (it measures the ability a material has to conduct heat) divided by density ρ and the specific heat capacity c_p .

$$D = \frac{k}{\rho c_p}$$

where

k is the thermal conductivity in $\frac{W}{m \cdot K}$

c_p is the specific heat capacity in $\frac{J}{kg \cdot K}$

ρ is the density in $\frac{kg}{m^3}$

Looking at this, the thermal diffusivity has the SI derived unit of $\frac{m^2}{s}$. However, for convenience, the unit that is usually used is $\frac{mm^2}{s}$ [1].

As mentioned above, thermography is a powerful tool when measuring thermal diffusivity. Thermography, also known as Thermographic testing, thermal imaging, infrared (IR) thermography is a non-destructive test that consists of obtaining thermal images that allow the visualization of temperature patterns on the surface of the material to be analyzed [2].

This can be done in a variety of ways. Figure 1 shows a summary of the different aspects to be considered when designing a thermographic inspection [3].

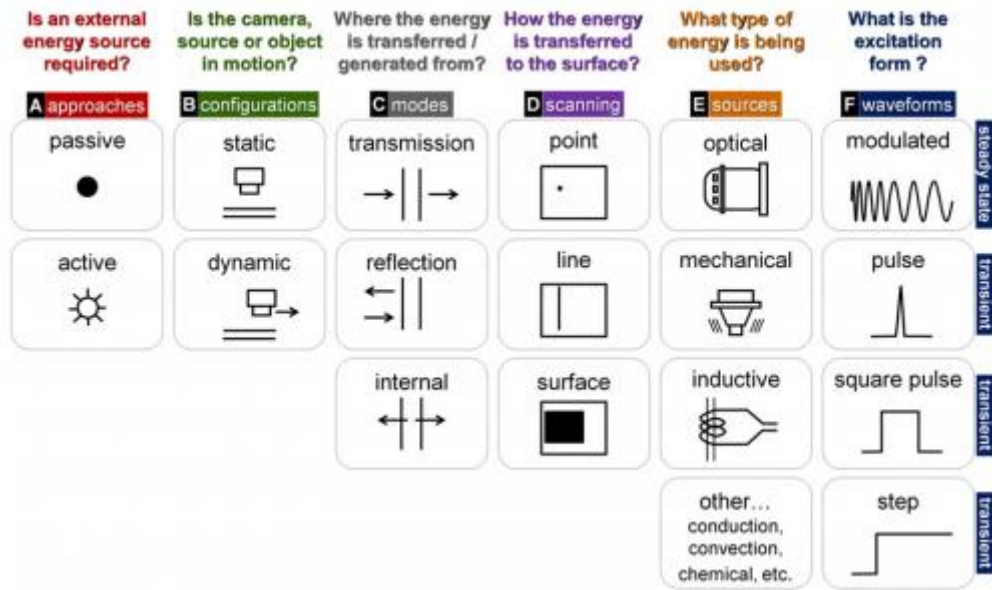


Figure 1 Aspects to be considered in a thermography inspection

It is organized in 6 columns. Each one represents an aspect to consider, and for these aspects there are different options that can be chosen to define how the thermographic inspection will be carried out. A brief explanation of each of the options will be given below.

Approaches: is an external energy source required? There are two options here:

- **Passive:** is characterized by the fact that the heat is not transmitted in a deliberate nor controlled way.
- **Active:** unlike in the previous case, in this case an additional stimulus is applied to raise the temperature of the object being analyzed so that the infrared camera can detect it.

Configurations: is the camera, the source, or the object in motion? There are also two options here:

- **Static:** Camera, Source and object remain static.
- **Dynamic:** is the opposite case for at least one of the three elements mentioned above.

Modes: where the energy is or generated from or transferred to? Three modes of work are presented here.

- **Reflection:** energy is delivered to the object from the same side as the camera.
- **Transmission:** in this case, the energy is delivered to one side of the object and the object is analyzed with the camera on the opposite side.
- **Internal:** in this case, the heat is generated internally in the object and is analyzed with the camera placed on either side of the object.

Scanning: how the energy is transferred to the surface? Here there are three

possibilities.

- **Point:** only one point of the sample is heated.
- **Line:** a line is heated in the desired direction along the object.
- **Surface:** in this case the entire surface of the object is heated at the same time.

Sources: what type of energy is being used?

- **Optical:** such as lasers or IR lamps.
- **Mechanical:** as sound or ultrasound.
- **Inductive:** as Eddy currents.
- **Other:** e.g. heating blankets for conduction heating of large aeronautical elements, or heating guns for convection heating of relatively small elements.

Waveforms: how the Surface is being stimulated?

- **Modulated:** the energy is modulated at a particular frequency.
- **Pulse:** a pulse of short duration, from microseconds to milliseconds.
- **Square pulse:** a pulse of long duration, several seconds or minutes.
- **Step:** continuous warm-up.

The use of each of these four options dictates the photothermal technique used.

- **Lock-in thermography (LT):** it is carried out in a dynamic steady-state. It consists of periodically heating the sample at a specific frequency to measure the amplitude and phase of the thermal response.
- **Pulsed Thermography (PT):** the purpose of delivering a short pulse of energy is to see how the defective areas of the sample cool at a different rate than those that are not defective.
- **Square Pulsed Thermography (SPT):** the difference with the previous one is that the pulse is longer, and the sample is monitored during heating and cooling.
- **Step Heating Thermography (SHT):** in this case the sample is heated continuously in order to analyze it only during heating, not during cooling.
- **Point or Line scan Thermography:** in this case the energy, the laser point for example, moves across the surface of the sample, while the camera records it at a specific distance.

This concludes the description of Thermography. Now the work will be put in context, and it will be explained why the technique used to take the measurements of the different materials' diffusivities has been chosen. It must be mentioned that there are methods for measuring diffusivity with a static laser beam (modulated [4], pulsed [5] or

step [6]). This has limitations because only a limited region is probed. To avoid these limitations, the aim of this work is to put together an experimental method to be able to probe large regions of the sample with a beam that scans the surface. This has many applications in the aerospace field, being able to scan large components of spacecrafts and determine any number of properties in a non destructive way is incredibly useful. The diffusivity can be measured this way, which as it has already been said is the aim of this work. Also, in the future, this technique will be used to detect and characterize cracks in those very same components. This will be discussed in the final section of this work.

The fact that large regions of a component are to be analyzed means that the spot of the laser must be in motion, with the component, or the sample of the material remaining static. This technique is called flying spot, first introduced over twenty years ago [7] [8] for the purpose of detecting cracks in materials, as mentioned above. The technology has improved over time and advances in optical control, lasers, and infrared cameras now allow this technique to be used to its best advantage. It can be used to measure thermal properties of materials [9].

So, after the previous considerations about thermography, we can classify the flying spot technique as shown in the following figure.

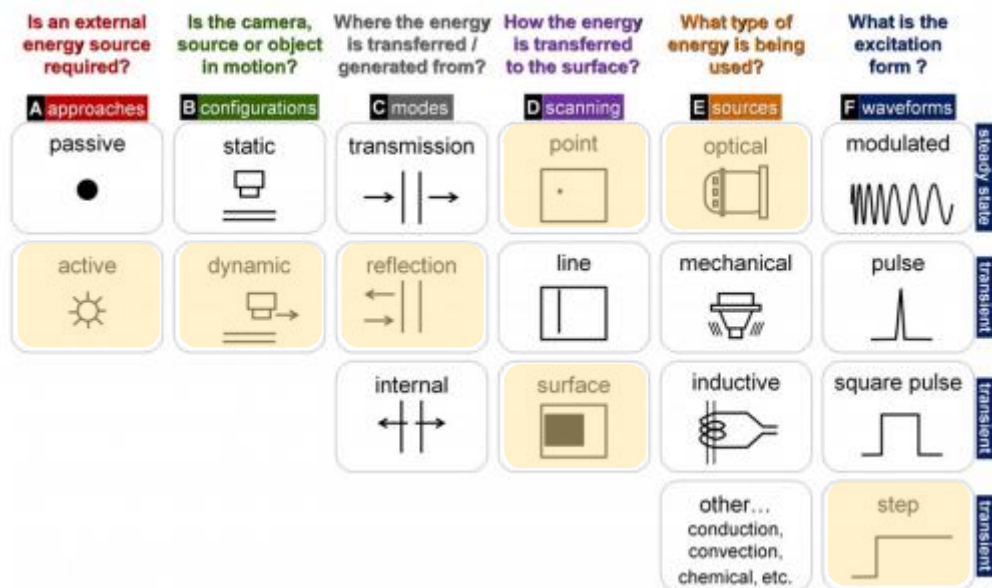


Figure 2 Relevant aspects to the flying spot thermography

As for the approach, it would be active, using an external energy source, the laser. The setting is Dynamic, because in our case, the laser will be in motion with the sample static. The mode is Reflection, because the laser and the camera are on the same side of the sample. The scanning method is point or spot, because a focus laser is used. The spot moves following a line across the surface of the sample and properties will be measured along that direction as well as the direction perpendicular to the laser motion. The source would be optical, as mentioned above a moving laser will be used to excite the sample. The waveform used is step, which determines that we use the SHT technique, for analyzing what happens during heating and as mentioned above, line scan thermography.

The following section will explain how to obtain the necessary equations to calculate value of the diffusivity.

2. Theory of flying spot thermography: laser in motion at constant speed

In this section [10] we calculate the temperature field of the surface of a sample traveled in a straight line by a laser at constant speed. A schematic of the situation is shown in the following figure.

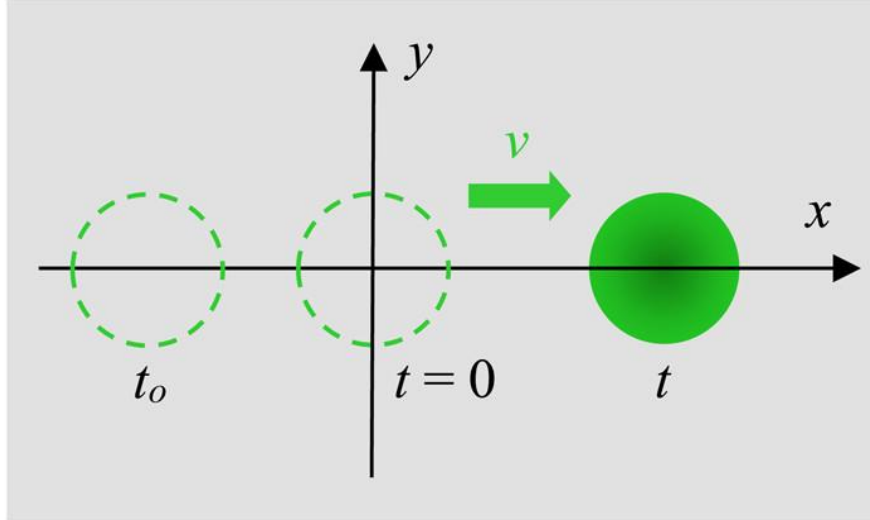


Figure 3 Schematic of the problem

The laser is turned on at t_0 and as mentioned above, it travels at a constant speed of v . It will pass through the origin of coordinates in $t = 0$. The purpose of calculating the temperature field is to be able to know the surface temperature of the sample at any time t .

Let the material be homogeneous, isotropic, semi-infinite and opaque. For the purposes of this following calculations the heat losses due to convection and radiation are disregarded.

The calculation starts considering that the material is briefly illuminated by a laser of power of P_0 at point $(b, 0, 0)$. The result is an increase in temperature with respect to the environment associated with an energy of $dQ_0 = P_0 dt$, a laser spot radius of a and the fraction of the energy absorbed by the sample of η . $\varepsilon = k/\sqrt{D}$ is the thermal effusivity which measures the ability of the material to exchange thermal energy with the surroundings. The temperature field in the material can be written as Eq. (1) [11]:

$$dT(x, y, z, t) = \frac{2\eta P_0}{\varepsilon\sqrt{\pi^3 t}} e^{-\frac{z^2 a^2 + 8Dt[(x-b)^2 + y^2 + z^2]}{4Dt(a^2 + 8Dt)}} \frac{1}{a^2 + 8Dt} dt \quad (1)$$

Now we introduce the condition that the laser moves along the x-axis with constant velocity v , obtaining Eq. (2). Then the temperature at any point (x, y, z) at a time t due to the effect of the energy transmitted by the laser in time τ is [11]:

$$dT(x, y, z, t) = \frac{2\eta P_0}{\varepsilon\sqrt{\pi^3}\sqrt{(t-\tau)}} \frac{e^{-\frac{z^2 a^2 + 8D(t-\tau)[(x-v\tau)^2 + y^2 + z^2]}{4D(t-\tau)(a^2 + 8D(t-\tau))}}}{a^2 + 8D(t-\tau)} d\tau \quad (2)$$

Note that for $t = 0$ the laser would be at the origin of coordinates.

To obtain the total temperature rise at any point (x, y, z) , the above expression is integrated taking into account that the laser is turned on from t_0 to t , obtaining Eq. (3) [11].

$$T(x, y, z, t) = \frac{2\eta P_0}{\varepsilon\sqrt{\pi^3}} \int_{t_0}^t \frac{1}{\sqrt{(t-\tau)}} \frac{e^{-\frac{z^2 a^2 + 8D(t-\tau)[(x-v\tau)^2 + y^2 + z^2]}{4D(t-\tau)(a^2 + 8D(t-\tau))}}}{a^2 + 8D(t-\tau)} d\tau \quad (3)$$

Now we particularize for the surface of the sample what the IR camera detects [11].

$$T(x, y, 0, t) = \frac{2\eta P_0}{\varepsilon\sqrt{\pi^3}} \int_{t_0}^t \frac{1}{\sqrt{(t-\tau)}} \frac{e^{-\frac{2[(x-v\tau)^2 + y^2]}{a^2 + 8D(t-\tau)}}}{a^2 + 8D(t-\tau)} d\tau \quad (4)$$

These equations represent the temperature evolution at any time since the laser is turned on. This evolution consists of a non-stationary period in which the temperature increases. This is followed by a stationary period at constant temperature.

Assuming a very tightly focused laser spot of radius $a = 0$, stationary state $t_0 = -\infty$ and laser at the origin of coordinates $t = 0$, the analytical solution of Eq. (3) is Eq. (5) [11]:

$$T(x, y, z, t) = \frac{2\eta P_0}{\varepsilon\sqrt{\pi^3}} \int_{-\infty}^0 \frac{1}{\sqrt{(t-\tau)}} \frac{e^{-\frac{(x-v\tau)^2 + y^2 + z^2}{4D(t-\tau)}}}{4D(t-\tau)} d\tau = \frac{\eta P_0}{2\pi k R} e^{-\frac{v(R+x)}{2D}} \quad (5)$$

Where $R = \sqrt{x^2 + y^2 + z^2}$. The following figure shows two representations of the natural logarithm of the temperature, calculated with Eq. (5). The material in question is AISI-304, with a thermal conductivity $k = 16 \frac{W}{mK}$ and a diffusivity of $D = 4 \frac{mm^2}{s}$. The laser speed is 2 cm/s .

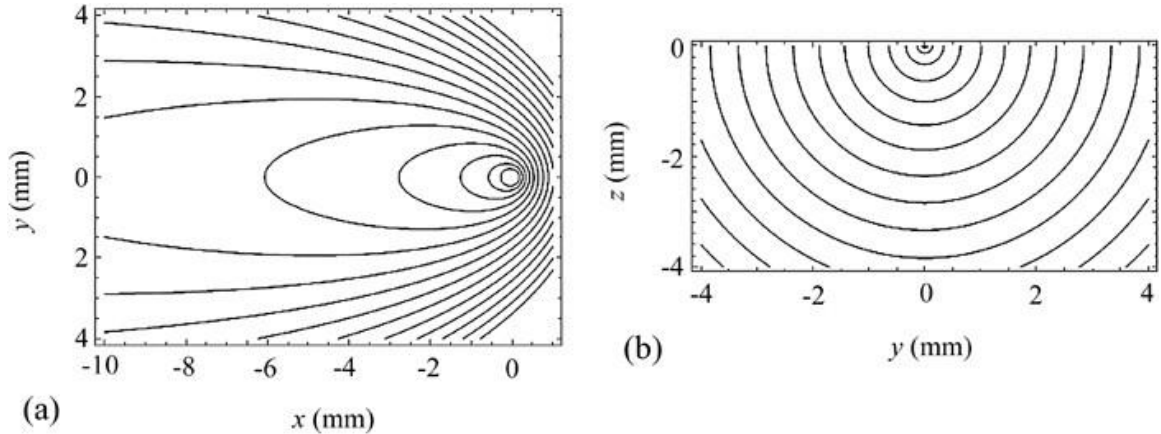


Figure 4 Representation of the calculated temperature distribution in steady-state for AISI-304. (a) Surface temperature and (b) $x=0$ section [11]

Fig. 4a shows the surface temperature $(x, y, 0)$. As can be seen the laser velocity induces a strong asymmetry in the surface temperature field, which increases with laser velocity, but decreases with diffusivity. This is not the case in the section $x = 0$ (Fig. 4b). Here the symmetry is always maintained as long as the material is isotropic.

Returning to Eq. (5), the temperature in the longitudinal direction (direction of laser motion) is Eq. (6) [11]:

$$T(x, 0, 0, t) = \frac{\eta P_0}{2\pi k} \frac{1}{|x|} e^{-\frac{v(|x|+x)}{2D}} \quad (6)$$

From this equation it can be inferred that the natural logarithm of the product of the temperature and the absolute value of the distance $\ln(T|x|)$ to the laser has a double linear relationship as a function of x . In front of the laser ($x > 0$) the slope of $\ln(T|x|)$ is Eq. (7) [11]:

$$m_x = -\frac{v}{D} \quad (7)$$

This equation will be used to calculate the diffusivity in the longitudinal direction of the sample. The information that can be obtained from behind of the laser will be discussed later.

Now in Eq. (5), we study what happens in the y , and z directions obtaining Eq. (8) and (9) [12].

$$T(0, y, 0, t) = \frac{\eta P_0}{2\pi k} \frac{1}{|y|} e^{-\frac{v(|y|)}{2D}} \quad (8)$$

$$T(0, 0, z, t) = \frac{\eta P_0}{2\pi k} \frac{1}{|z|} e^{-\frac{v(|z|)}{2D}} \quad (9)$$

From these two equations it is inferred that $\ln(T|y|)$ and $\ln(T|z|)$ behave linearly as a function of the distance to the laser with the same slope obtaining Eq. (10) [12].

$$m_y = m_z = \pm \frac{v}{2D} \quad (10)$$

This is the other equation to be used, in this case to calculate the transverse diffusivity.

The following figure shows the representations of $\ln(T|x|)$, $\ln(T|y|)$ and $\ln(T|z|)$ for AISI-304.

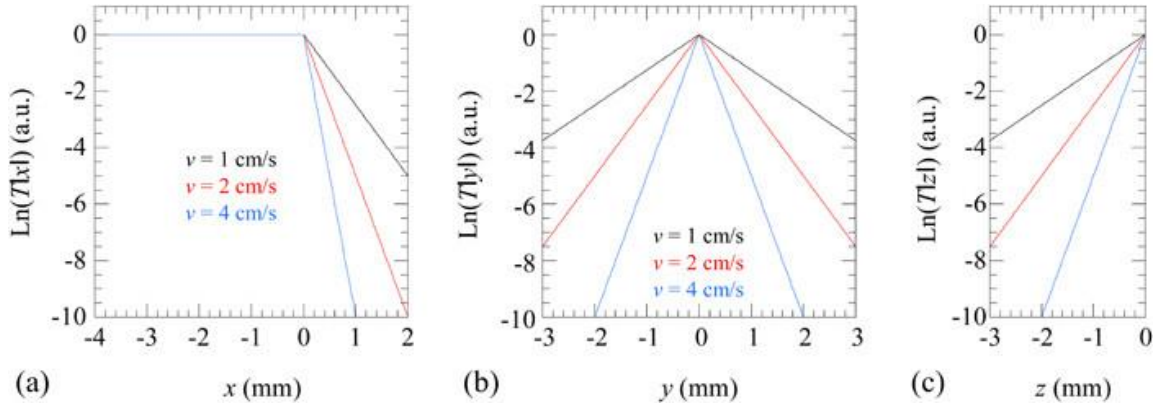


Figure 5 Representation of the natural logarithm of the temperature times the distance to the laser spot. (a) longitudinal profile, (b) transverse profile and (c) depth profile [12]

It should be mentioned that these linearities are only valid when the steady state has been reached. As can be seen, the calculation of the diffusivity is simple, but for isotropic materials, it is more reliable to use the transverse profile. Due to the symmetry of its branches, a larger number of data can be used before reaching the noise level. Finally, it should be noted that for a laser radius of $a \neq 0$, which is what happens in reality, there will be a rounded shape in the graphs at the point where the laser is located.

Returning to what was mentioned above about what happens behind the laser, the best way to explain it is to look at the following figure.

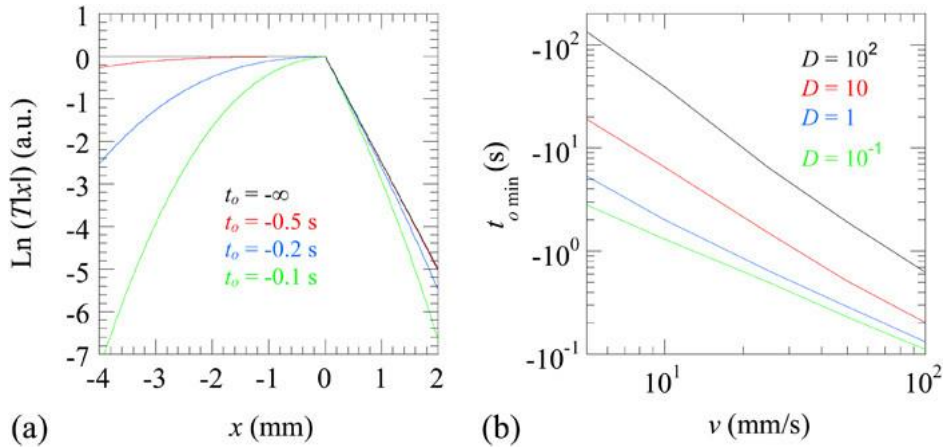


Figure 6 The longitudinal profile at different times. (a) difference in the graph when switching the time at which the laser is turned on and (b) minimum time to reach the steady state for different diffusivity values [12]

This part, being flat, does not give any information about the diffusivity, but it does give information about the steady state. It indicates whether the stationary state has been reached and the quality of the measurement. In Fig. 6a the longitudinal profile $\text{Ln}(T|x|)$ can be seen, for AISI-304, with $a = 0$, $v = 1 \text{ cm/s}$ and the laser at the coordinate origin $x = 0$. The time at which the laser is turned on changes. It follows that the greater the absolute value of t_0 is, the temperature will be that much closer to the steady state. In other words, when that part of the graph is completely flat, the steady state has been reached. In in Fig. 6b it is shown, for different diffusivities, the minimum time required to reach the steady state, $t_{0,min}$, as a function of the laser velocity. It can be seen that this minimum time in absolute value decreases with increasing laser speed but also increases with the diffusivity of the material.

3. Experimental device

3.1 Setup

Fig. 7 shows the scheme of the setup used to perform all the measurements presented in the next section. The setup was developed in such a way that the laser spot is in motion while the sample remains static.

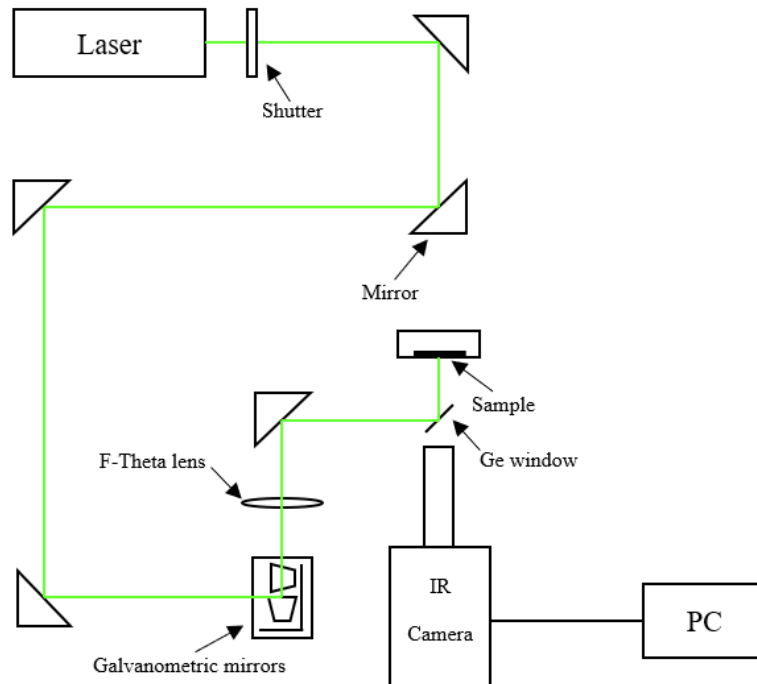


Figure 7 Scheme of the experimental setup

First of all, there is a Verdi V6 laser with a wavelength of 532 nm and a power up to 6W.

Then there is a shutter which allows to illuminate the sample or to cut the illumination at will. The shutter is mainly used in pulsed mode, since being controlled by the flying spot software, it can be opened and close however the user programs it to. Although the software has its limitations, as will be explained in more detail further along in this section.

After that a set of mirrors is necessary to direct the laser in the desired direction, that of the galvanometric mirrors and the F-Theta lens. Figure 8 shows this part of the set up.



Figure 8 The galvanometric mirrors and the F-Theta lens [13]

The galvanometric mirrors are used to move the laser spot. There are two of them, one moves the spot along the vertical direction and the other along the horizontal direction. This movement is accomplished by applying a specific amount of voltage to these mirrors. This means that the movement they produce is not continuous, is discrete. This will have its consequences in the measurements, which will be discussed later on.

The laser beam enters and leaves the mirrors collimated and unfocused. In this technique the laser must be focused on the sample. To avoid this a focusing lens must be placed, the F-Theta lens. The following figure shows different types of lenses as a means to explain why the F-Theta lens is used for this.

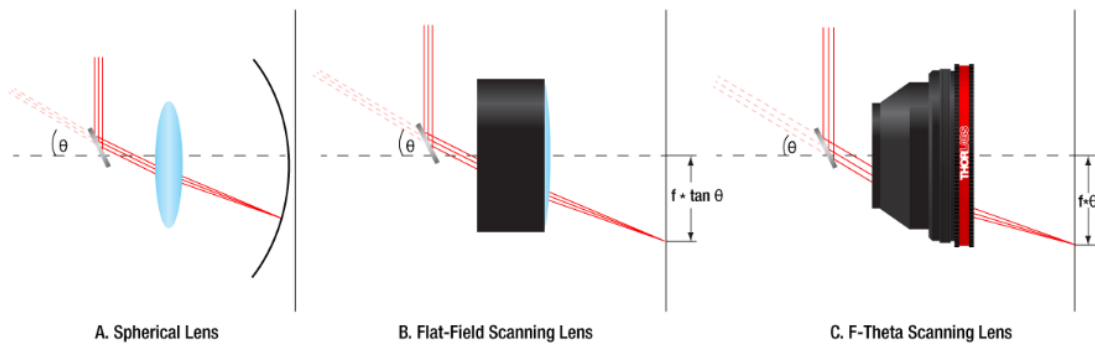


Figure 9 a) spherical lens, b) Flat-Field scanning lens and c) F-Theta lens

A spherical lens can only provide an image along a circular plane which is not what this experiment is about. A planar image is needed. This could be solved by placing a Flat-Flied scanning lens. The problem with this one is that the displacement of the laser beam (caused by the galvanometric mirrors) is dependent on the product of the focal length f and the tangent of the displacement angle θ . Although this non-linear relation could be accounted for with an algorithm, the simplest solution is to use a F-Theta lens.

F-Theta lenses are designed to produce a linear displacement of the laser beam, the product of the focal length f and the displacement angle θ . This lens also provides a planar focusing plane with an almost constant laser spot. The linearity of this displacement means that the position of the laser is directly proportional to the scan angle changed by the galvanometric mirrors [14] [13].

Another simple mirror directs the laser beam to the Ge window. This reflects the visible light and is transparent to the IR wavelengths, preventing the scattered laser radiation to reach the IR camera [9].

Finally, there is the IR camera which records the temperature field at the surface of the sample. This is a FLIR SC7500 model, 320x256 pixels, pitch of 30 μm and a Noise Equivalent Temperature Difference (NETD) of 20 mK. Another important matter is that the camera has a macro lens with a special resolution of 30 μm . This was put so that an object in the focal plane of the lens, a 30 μm square for instance, is also a 30 μm square in the image plane, which is the position the detector of the camera is at. This means the angular magnification is 1.

3.2 How to perform a measurement

Two software are used to perform a measurement, the flying-spot software and Altair software. The former, as mentioned above, controls the movement of the galvanometric mirrors by applying a certain of voltage to them. The latter is the recording software, which will produce a movie that the user can draw information from.

The flying spot software is explained in detail in Appendix I. Since Altair software is more than 20 years old, it was deemed unnecessary to describe in this work. Now the most relevant parameters for the measurement will be discussed, as well as the limitations this set up has. This is vital when performing the measurement, we want. These limitations are tight to both the equipment itself and the flying spot software. This means that there isn't total freedom when it comes to performing a measurement. Also, having in mind a certain doable measurement, one most know how to program it in the flying spot software. This is because the software has some glitches, so it isn't as simple and intuitive as it seems.

This is also explained in detail in Appendix I, but all this will be quickly mentioned in this section too because is relevant for the results presented in the next section and to understand why those parameters were chosen for measurements and not different ones.

First the glitches the flying spot software has will be discussed and how the failure to avoid these can affect the measurement. To do this, all the sections of the software will be briefly described. The next figure shows how the interface of the software is divided.

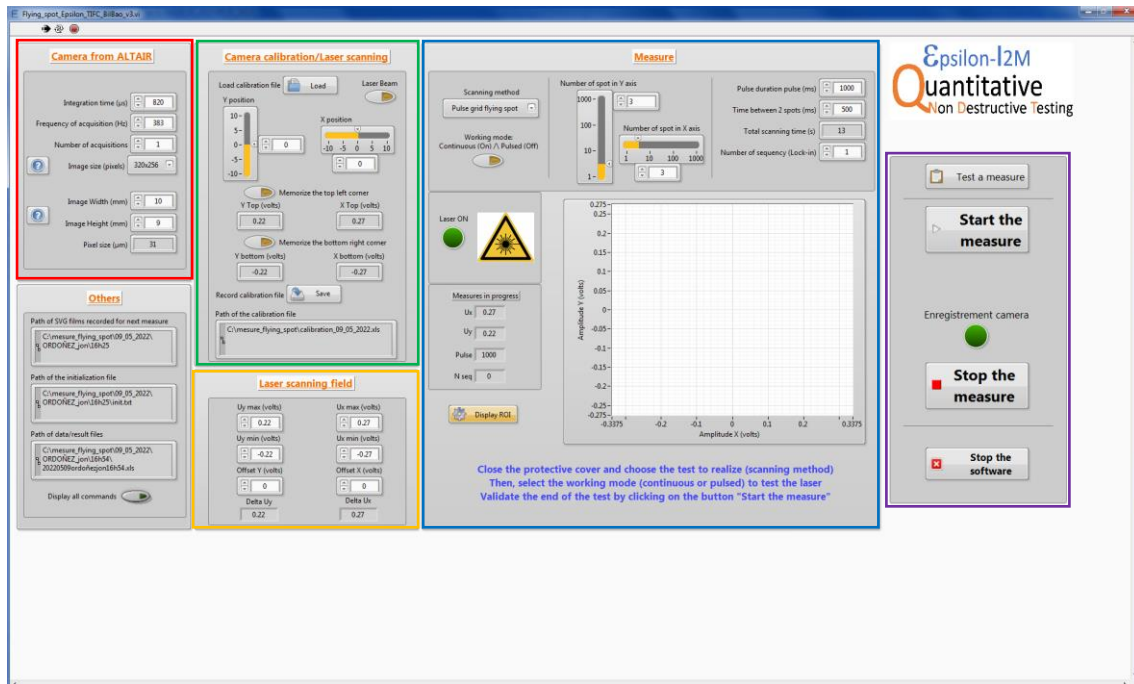


Figure 10 Flying spot software interface

Camera from ALTAIR

This is the section where all the pertinent information from Altair software regarding the camera is input. This section has a glitch when it comes to writing the size of the image. Since the software only admits integer numbers, whatever number is written, the software will round it up to an integer number. The pixel size is displayed. Regardless, the user must input the width and height of the field of view (FOV) of the camera.

Camera Calibration/Laser Scanning

In this Camera calibration/Laser scanning section, the user will input the range of voltages that need to be applied to the mirrors so that the laser spot scans the field of view of the camera. There are no glitches in this section, for more information refer to Appendix I.

Laser scanning field

In this Laser scanning field section, the user determines the limits of the field the spot will be moving in. This field can be larger or smaller than the camera field previously calibrated. The camera field won't change because the camera is always the same. However, this scanning field may change from one measurement to another. As with the previous one, there are no glitches here, see Appendix I for more information.

Measure

In this Measure section, the user will determine various parameters of the measurement. First notable glitch to mention is regarding the working modes and the displayed durations. Evidently, the main difference between these modes is that the shutter stays open in continuous mode and it opens and closes in pulsed mode. The other important difference is how the durations work. Basically, in pulsed mode the shutter will open for the specified amount of time input as *Pulse duration*, and it will close for the amount of time input in *Time between 2 spots*. In continuous it will stay always opened. So, in

continuous mode however long the measurement is, that duration must be divided by two and entered separately in Pulsed duration and Time between 2 spots.

This wouldn't be a problem if it weren't for the following glitches.

First, the 'Total scanning time' displayed in each mode is different and it doesn't match the real duration in neither case. This has also to do with the number of spots. In pulsed working mode it'll display a time equal to number of spots x (pulse duration + time between 2 spots) – 1 x time between 2 spots. In continuous working mode the displayed time is number of spots x pulse duration. In neither case the displayed time matches the real duration of the measurement, so it's important to keep in mind and know how long the measurement will take regardless of what this software says. This will be important when setting the duration of the movie.

The second glitch has to do with continuous mode. When on pulsed mode, there's no problem. Enter the values and it'll function correctly. But when working on continuous mode, the parameters must be introduced in pulsed mode first. Once they are introduced and ready to go as if working on pulsed working mode, change the mode to continuous. The values will change, and the user must enter them again, now in continuous. For unknown reasons if not done in this manner the measurement won't work properly.

Both these glitches must be carefully avoided, or the duration of the measurement will not be the desired one. No more glitches on this section.

Now that the glitches are explained, the limitations this whole set up has will be discussed.

The first limitation is that the galvanometric mirrors move discretely, meaning each amount of voltage, will make them move a certain angle, then stop and move that same distance again. This movement happens each time the previously mentioned Time between 2 spots ends. The velocity of the movement itself, albeit extremely high, is unknown. So, even on continuous mode the sequence is, Pulse duration + Time between 2 spots, then move, then start again. This is noticeable in the resulting measurements as will be shown later on.

The second limitation is that in both Pulse duration and Time between 2 spots, the minimum admitted duration is 20 milliseconds. This has a direct impact in the desired velocity for the spot movement. This means that the lesser the number of spots, since the time the laser spot will stay in those spots is limited, the mirrors must move a greater distance. Which makes for a poor continuous measurement.

And the third limitation is the number of spots. The software admits a maximum of 1000 spots. Another fact to have in mind when choosing the velocity.

All this will be further discussed in the following section when analyzing the results.

4. Results of the experimental measurements

4.1 Analysis procedure

The procedure for taking and analyzing each of the measurements presented in this section was the same. First, a frame of what the IR camera was seeing was captured. Then, a movie was recorded while the laser was scanning the surface, following the steps described in Appendix I. These are movies showing infrared imaging of the laser spot moving on the surface of the sample, with the corresponding temperature changes in each pixel of the movie, thermograms. Then using Altair software, the frame initially taken was subtracted from each frame of that movie. This was done to eliminate the effect of emissivity differences and the Narcissus effect which occurs when the detector from the camera detects its own radiation reflected back by the sample. The result of this subtraction was a background-free movie.

These last movies are what have been analyzed. To do this, those movies must be converted to MATLAB format via the script in Appendix II introducing the total frames the movie has. Then using the script in Appendix III, the velocity of the spot is obtained, which will be needed in the calculation of the numerical value of the diffusivity, according to Eq. (7) and (10). This is done by entering the frames per second of the movie (fps) and both the number of the first and last frames in which the spot is visible in the movie. The script, after converting the frames to millimeters, performs a linear regression and the velocity is obtained. The reason the velocity needs to be calculated is because of all the limitations mentioned in previous sections, the actual velocity is not going to match the intended velocity.

As said before, there isn't total freedom when choosing the velocity due to the restrictions the flying spot software has. And even when choosing a velocity that the software can handle, since all the work has been done in continuous mode, the discrete movement of the laser spot and the time it takes for the mirrors to move have an impact on the real velocity. This time may be extremely short but over the course of the measurement it adds up. In the next table certain velocities are presented. These velocities are from other works previously done. The aim was to use those same velocities for this work. Besides each velocity are the values that need to be entered in the flying spot software to obtain those velocities.

Table 1 Intended velocities for the laser spot and the corresponding parameters for the flying spot software

v (mm/s)	d (mm)	t (s)	ts (ms)	ns
0.49	30	61.2244898	40	1530.61224
0.5	30	60	40	1500
1	30	30	40	750
4	30	7.5	40	187.5
4.3	30	6.97674419	40	174.418605
5.5	30	5.45454545	40	136.363636
10.9	30	2.75229358	40	68.8073394
21.4	30	1.40186916	40	35.046729
41.2	30	0.72815534	40	18.2038835
60.4	30	0.49668874	40	12.4172185
81.6	30	0.36764706	40	9.19117647

Knowing the velocity v that is intended for the laser and the fact that the sample is 30 millimeters long d , the time t it takes for the laser to scan the whole length of the sample is calculated. Since the aim is to move the laser in the most continuous manner possible, the time it stays in each spot must be the minimum possible. As was explained above this time is the sum of *Pulsed duration* and *Time between 2 spots*. The minimum the software admits in both cases is 20 milliseconds. This gives a total time in each spot (ts) of 40 milliseconds, as it can be seen in the table. Besides these two durations the number of spots also needs to be entered in the software (ns). This was calculated by dividing the total time and the time in each spot. The values in table 1 are the theoretical values that if introduced in the flying spot software, would produce the velocities shown in the first column. This means that if the introduced number of spots is 750, *Pulse duration* is 20 ms and *Time between 2 pulses* is 20 ms, the total duration of the measurement would be 30 s and the achieved velocity would be 1 mm/s.

Much of the obtained number of spots can't be introduced in the software. Some because they exceed the 1000 number of spots limit and others because the number of spots must be an integer number. So, in a way, table 1 gives information on whether or not those velocities are possible to obtain having all the flying spot software's restrictions in mind. Table 2 shows the modifications done having in mind both facts mentioned above, the time in each spot must be minimum and the number of spots maximum possible, the aim being to obtain velocities as close as possible to those of Table 1.

Table 2 Velocities and parameter to be entered in the flying spot software

ns	ts (ms)	t (s)	d (mm)	v (mm/s)
1000	61	61	30	0.49180328
1000	60	60	30	0.5
750	40	30	30	1
188	40	7.52	30	3.9893617
174	40	6.96	30	4.31034483
136	40	5.44	30	5.51470588
69	40	2.76	30	10.8695652
35	40	1.4	30	21.4285714
18	40	0.72	30	41.6666667
12	41	0.492	30	60.9756098
9	41	0.369	30	81.300813

Both velocities requiring 1500 number of spots were changed to 1000, and all the others were rounded to an integer number. Then following the same process as the table 1 but in reverse, the velocities that the laser spot is expected to achieve have been calculated. This aren't much different from the intended ones in Table 1. So, Table 2 not only gives information about the parameters that need to be entered in the software to achieve a certain velocity, but also about the duration the measurement will have, to which 2 seconds must be added when setting the recording time, as explained before. But as said before the real velocity will be calculated in MATLAB with the scrip in Appendix III, which will be used to calculate the diffusivity.

Looking at Eq. (7) and (10) is apparent that the slope of $\ln(T|x|)$ and $\ln(T|y|)$ representations is needed to calculate the diffusivity, as explained above. Ideally, via MATLAB, after a frame is chosen, the data from the longitudinal profile (profile in the direction of the movement of the laser spot) and the corresponding transverse profile (profile perpendicular to the motion) containing the laser spot would be plotted and analyzed. The problem is, the measurement is rather noisy, enough for the calculation of the needed slope to be inaccurate. The following figure shows two graphs, each corresponding to the longitudinal and transverse profiles respectively, for a single frame. The material is AISI-304 and the laser power is 1 W.

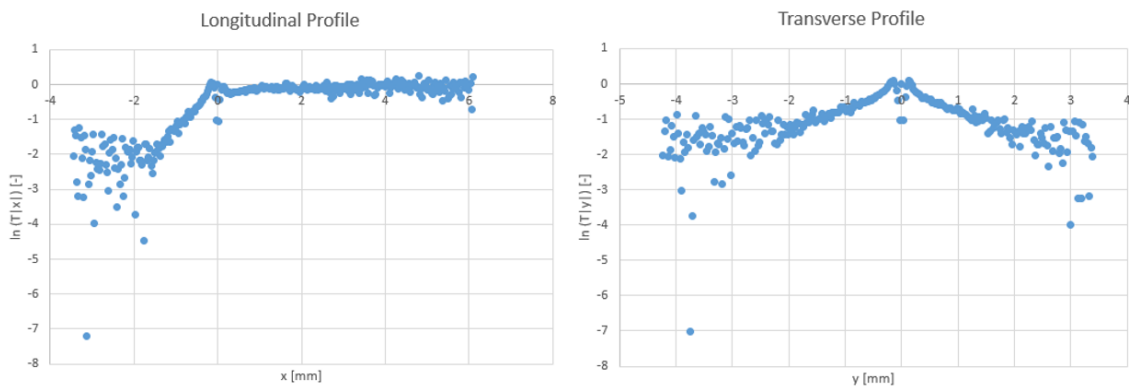


Figure 11 Graphs of the natural logarithm of the temperature times the distance to the laser spot for the longitudinal and transverse profiles of a single laser spot position for AISI-304 at 1 W

It is apparent that in the non-flat part of the graph corresponding to the longitudinal profile and in both branches of the graph corresponding to the transverse profile are quite noisy. This must be reduced in order to have more points to work with so a more accurate value of the slope can be calculated and consequently, a more accurate diffusivity. To do this, various profiles from different positions (frames) have been averaged. When averaging the longitudinal profiles, only those points (values along the x axis) that belong to all the profiles must be considered, the others must be discarded. So, the number of frames that can be averaged is limited by the position of the laser spot in the last profile. Only the points ahead of the laser are used to calculate the slope, so all the previous profiles before the last one contains those points, but the last one doesn't have as many points as the second to last one etc. A direct consequence of this is that if too many profiles are averaged, the flat part will begin to stop being flat and tend to go up. So, for the longitudinal profile only a few positions or frames are averaged. For the transverse profile there is no problem when it comes to averaging, the whole length of the movie in which the laser spot is captured can be averaged. Another important matter to mention is that the laser was already heating the sample to ensure that when it enters the camera's FOV, the steady state had already been reached. Figure 12 shows the graphs corresponding to the average of the longitudinal profile of four consecutive laser spot positions and the whole length for the transverse profile.

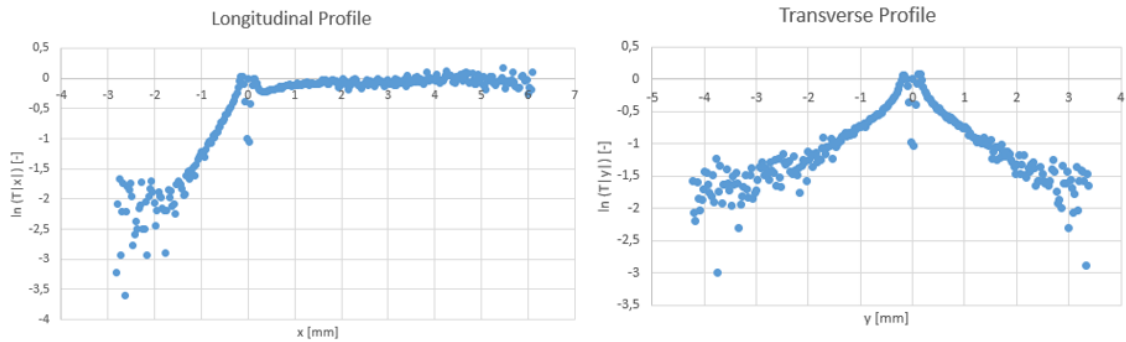


Figure 12 Graphs of the natural logarithm of the temperature times the distance to the laser spot for the average of the longitudinal profile of four consecutive laser spot positions and transverse profile for the whole length

Comparing these averaged graphs to the previous one is apparent that just with averaging four profiles, the noise is remarkably reduced, giving more points to work with. This has been done with all the measurements using the script in Appendixes IV and V depending on the profile being longitudinal or transverse respectively. Then the averaged data is converted to Excel format and plotted. The graphs above are the result of doing this. The last step is to calculate the slope, which can be easily done with Microsoft Excel by selecting the section of the graph and having Excel do a trend line and then show its equation from where the slope's value can be read. Using Eq. (7) and (10), the diffusivity value is obtained.

Now the measurements for each material will be presented.

4.2 Measurement results

In this section the results (thermograms, averaged profiles graphs and diffusivities) of the measurement for a single velocity of each material are shown. At the end there will be a summary with all the calculated diffusivities for all materials at all the velocities.

4.2.1 AISI-304, 5.17 mm/s at 1 W

The parameters used in the flying spot software are displayed in Table 3:

Table 3 Flying spot software parameters for AISI-304, 5,17 m/s

Intended v (mm/s)	ns	ts (ms)	t (s)	Possible v (mm/s)
5.5	136	40	5.44	5.51

A frame of the resulting thermogram after having subtracted the corresponding initial frame is shown in Fig. 13:

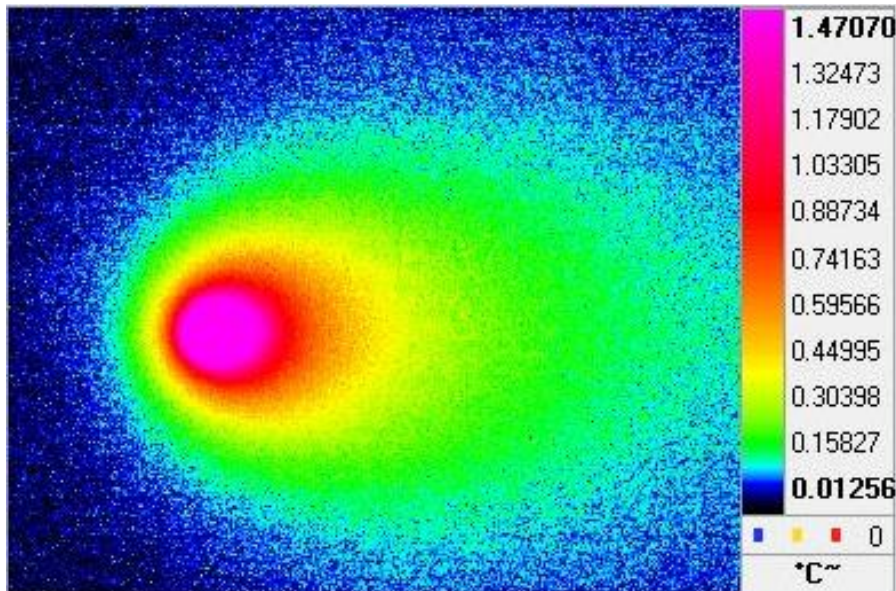


Figure 13 Thermogram corresponding to AISI-304, 5,17 mm/s at 1 W

Length of the movie: 700 frames

Interval of laser spot captured by the camera: from 178 to 358 frames

Real velocity: 5.17 mm/s.

Averaged longitudinal profiles: from 294 to 306 frames

Averaged transverse profiles: from 178 to 358.

The resulting graphs are shown in Fig. 14 and 15:

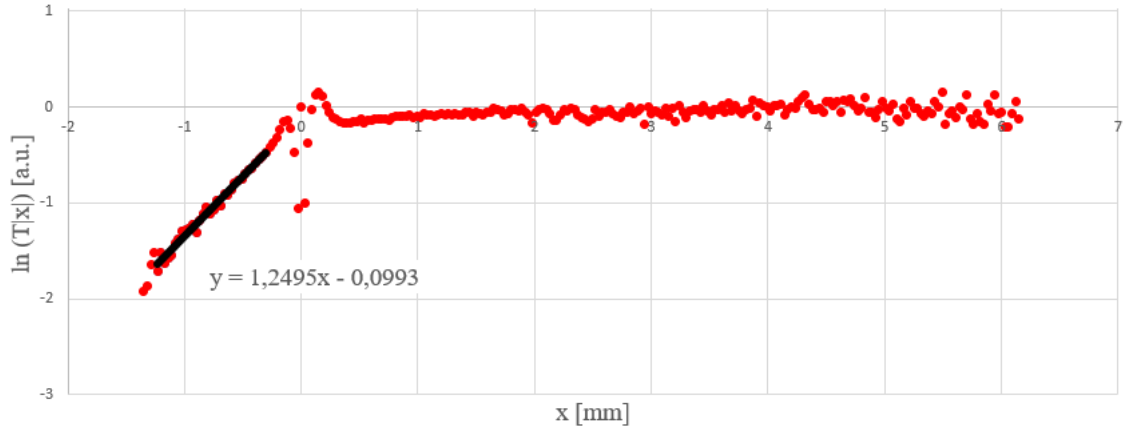


Figure 14 Averaged longitudinal profiles from frames 294 to 306 of AISI-304, 5.17 mm/s at 1 W

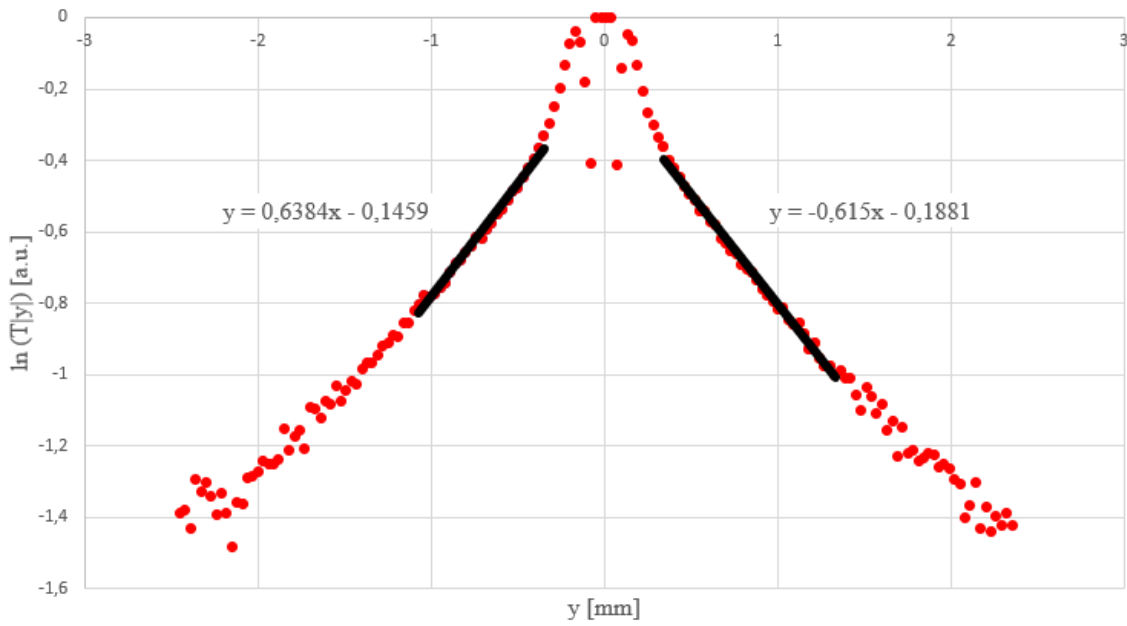


Figure 15 Averaged transverse profiles from frames 178 to 358 of AISI-304, 5.17 mm/s at 1 W

Fig. 14 and 15 represent the averaged longitudinal (from frame 294 to 306) and transverse profiles (from frame 178 to 358) respectively, of AISI-304 with a velocity $v = 5.17 \text{ mm/s}$ at 1 W . In Fig. 14 is shown that the slope is equal to 1.25 and in Fig. 15 the shown slopes are 0.64 and -0.62 in each branch.

The diffusivity of the longitudinal profile is obtained from Eq. (7):

$$D = 4.13 \frac{\text{mm}^2}{\text{s}}$$

The diffusivities on both right and left branches of the graph of the transverse profile are obtained from Eq. (10):

$$D_l = 4.05 \frac{\text{mm}^2}{\text{s}}$$

$$D_r = 4.20 \frac{\text{mm}^2}{\text{s}}$$

4.2.2 PEEK, 0.91 mm/s at 0.01 W

The parameters used in the flying spot software are displayed in Table 4:

Table 4 Flying spot software parameters for PEEK, 0.91 mm/s

Intended v (mm/s)	ns	ts (ms)	t (s)	Possible v (mm/s)
1	750	40	30	1

A frame of the resulting thermogram after having subtracted the corresponding initial frame is shown in Fig. 16:

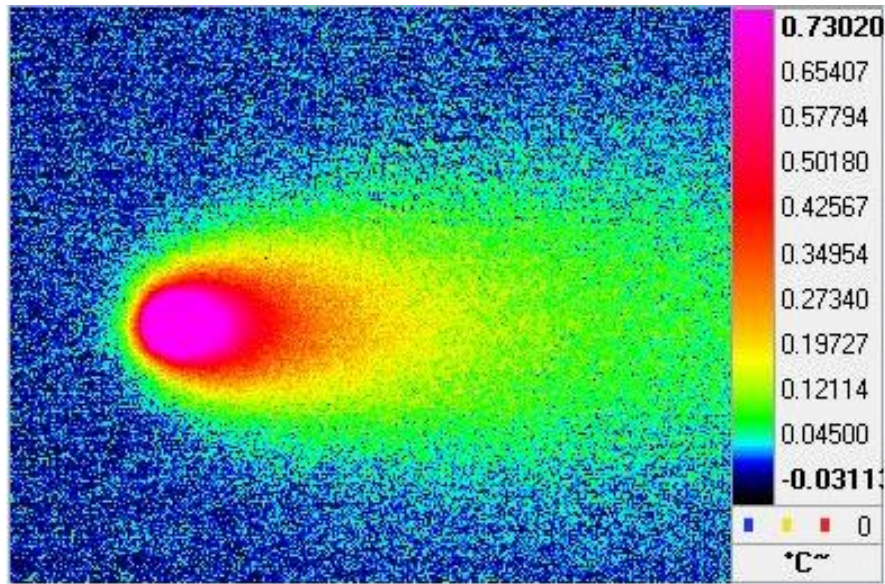


Figure 16 Thermogram corresponding to PEEK, 0.91 mm/s at 0.01 W

Length of the movie: 3200 frames

Interval of laser spot captured by the camera: from 860 to 1760 frames

Real velocity: 0.91 mm/s.

Averaged longitudinal profiles: from 1600 to 1612 frames

Averaged transverse profiles: from 860 to 1760 frames

The resulting graphs are shown in Fig. 17 and 18:

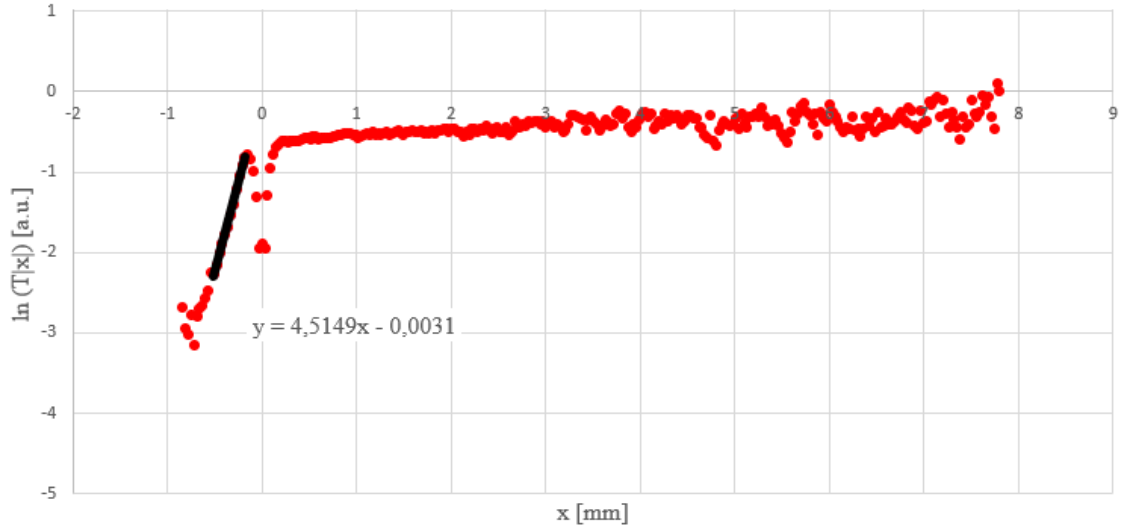


Figure 17 Averaged longitudinal profiles from frames 1600 to 1612 of PEEK, 0.91 mm/s at 0.01 W

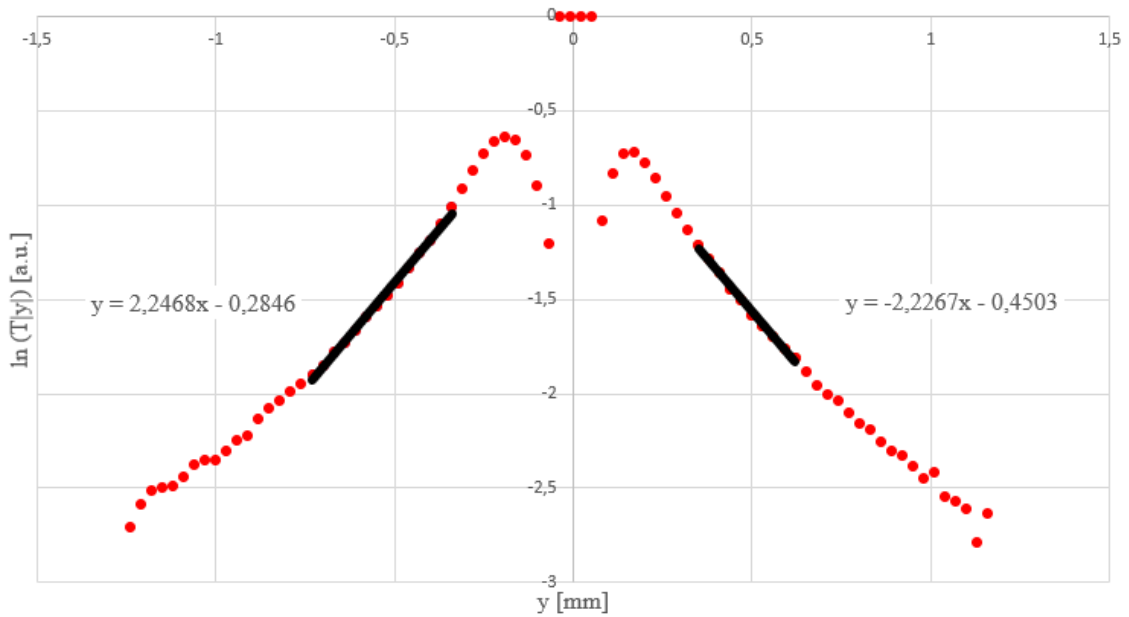


Figure 18 Averaged transverse profiles from frames 860 to 1760 of PEEK, 0.91 mm/s at 0.01 W

Fig. 17 and 18 represent the averaged longitudinal (from frame 1600 to 1612) and transverse profiles (from frame 860 to 1760) respectively, of PEEK with a velocity $v = 0.91$ mm/s at 0.01 W. In Fig. 17 is shown that the slope is equal to 4.51 and in Fig. 18 the shown slopes are 2.25 and -2.23 in each branch.

The diffusivity of the longitudinal profile is obtained from Eq. (7):

$$D = 0.20 \frac{\text{mm}^2}{\text{s}}$$

The diffusivities on both right and left branches of the graph of the transverse profile are obtained from Eq. (10):

$$D_l = 0.20 \frac{mm^2}{s}$$

$$D_r = 0.20 \frac{mm^2}{s}$$

4.2.3 Glass, 3.78 mm/s at 0.01 W

The parameters used in the flying spot software are displayed in Table 5:

Table 5 Flying spot software parameters for glass, 3.78 mm/s

Intended v (mm/s)	ns	ts (ms)	t (s)	Possible v (mm/s)
4	188	40	7.52	3.99

A frame of the resulting thermogram after having subtracted the corresponding initial frame is shown in Fig. 19:

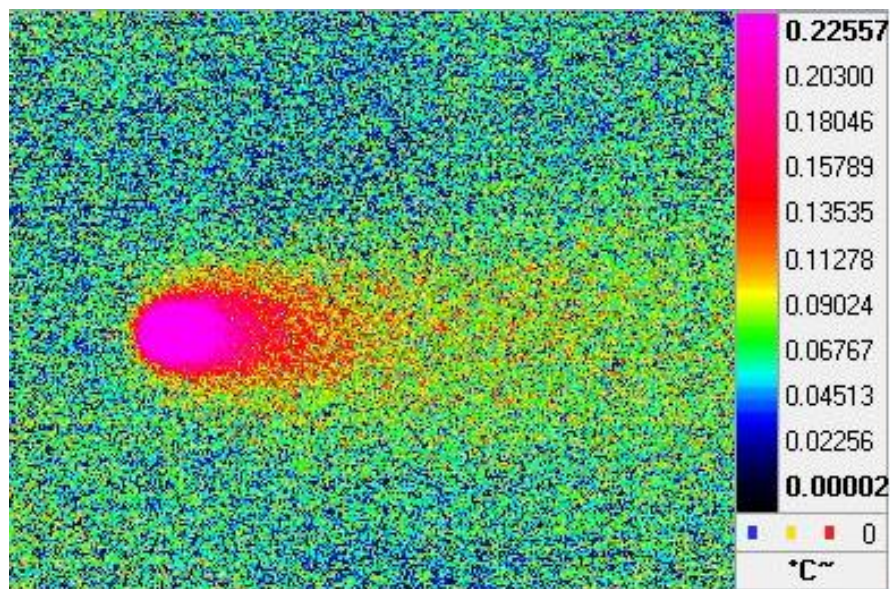


Figure 19 Thermogram corresponding to glass, 3.78 mm/s at 0.01 W

Length of the movie: 1000 frames

Interval of laser spot captured by the camera: from 220 to 440 frames

Real velocity: 3.78 mm/s.

Averaged longitudinal profiles: from 400 to 412 frames

Averaged transverse profiles: from 220 to 440 frames

The resulting graphs are shown in Fig. 20 and 21:

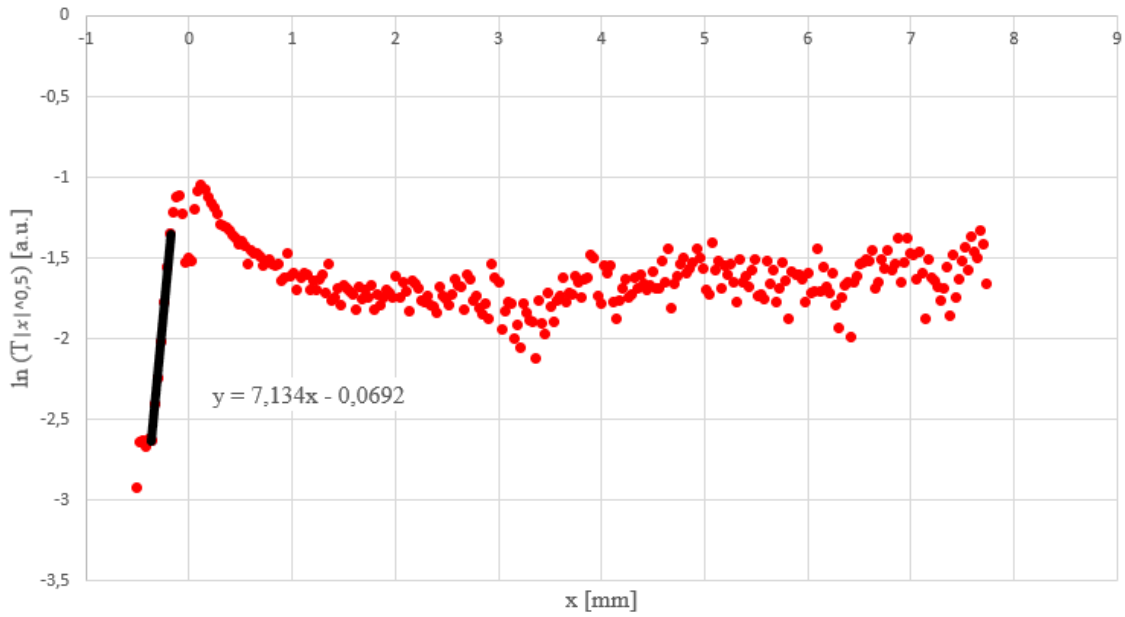


Figure 20 Averaged longitudinal profiles from frames 400 to 412 of glass, 3.78 mm/s at 0.01 W

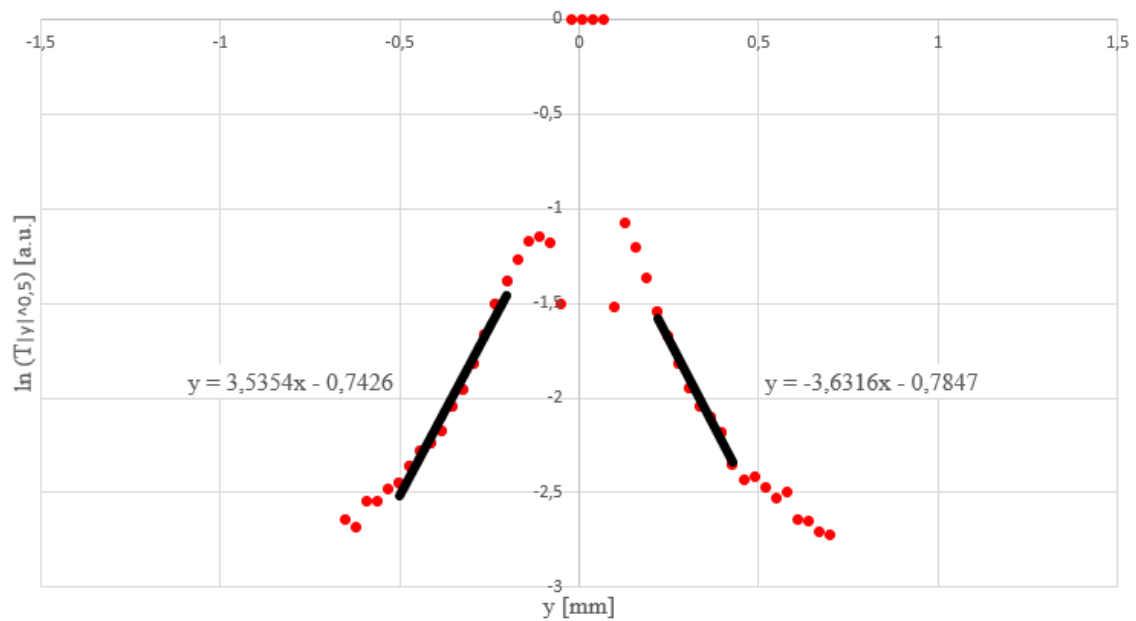


Figure 21 Averaged transverse profiles from frames 220 to 440 of glass, 3.78 mm/s at 0.01 W

Fig. 20 and 21 represent the averaged longitudinal (from frame 400 to 412) and transverse profiles (from frame 220 to 440) respectively, of glass with a velocity $v = 3.78$ mm/s at 0.01 W. In Fig. 20 is shown that the slope is equal to 7.13 and in Fig. 21 the shown slopes are 3.54 and -3.63 in each branch.

The diffusivity of the longitudinal profile is obtained from Eq. (7):

$$D = 0.53 \frac{\text{mm}^2}{\text{s}}$$

The diffusivities on both right and left branches of the graph of the transverse profile are obtained from Eq. (10):

$$D_l = 0.53 \frac{mm^2}{s}$$

$$D_r = 0.52 \frac{mm^2}{s}$$

Table 6 shows all the diffusivity results measured for AISI-304 at different velocities:

Table 6 Diffusivity results for AISI-304 at different velocities

Sample	Velocity (mm/s)	D (mm ² /s) (Longitudinal profile)	D _l (mm ² /s) (Transverse profile)	D _r (mm ² /s) (Transverse profile)	D (mm ² /s) (Literature [15] [16])
AISI-304	5.17	4.13	4.05	4.20	4.0
AISI-304	10.2004	4.15	4.13	3.04	4.0

Table 7 shows all the diffusivity results measured for PEEK at different velocities:

Table 7 Diffusivity results for PEEK at different velocities

Sample	Velocity (mm/s)	D (mm ² /s) (Longitudinal profile)	D _l (mm ² /s) (Transverse profile)	D _r (mm ² /s) (Transverse profile)	D (mm ² /s) (Literature [15] [16])
PEEK	0.4548	0.20	0.20	0.20	0.18
PEEK	0.9097	0.20	0.20	0.20	0.18
PEEK	3.6369	0.29	0.24	0.24	0.18

Table 8 shows all the diffusivity results measured for glass at different velocities:

Table 8 Diffusivity results for glass at different velocities

Sample	Velocity (mm/s)	D (mm ² /s) (Longitudinal profile)	D _l (mm ² /s) (Transverse profile)	D _r (mm ² /s) (Transverse profile)	D (mm ² /s) (Literature [15] [16])
Glass	0.4695	0.5	0.52	0.53	0.5-0.6
Glass	0.9405	0.5	0.52	0.52	0.5-0.6
Glass	3.7787	0.53	0.53	0.52	0.5-0.6

5. Conclusions and future work

This work has covered the experimental procedure and the results of performing diffusivity measurements on various materials using the flying spot technique. The problem is that the flying spot software, besides all the glitches, also has limitations. The most important limitation of the system is the inability to move the laser quickly (high speeds, typically for high diffusivity materials) in a quasi-continuous way. This makes the device unsuitable for working with high diffusivity materials. For this type of materials, it might be better to analyze different positions of the surface by exciting them with a pulsed or modulated laser, in order to see eventual inhomogeneities. The obtained results are accurate enough looking at the real results from the literature but working with a velocity any higher than those presented in this work leads to poor measurements.

The next step to this would be the detection and characterization of crack in the materials. A crack in the material produces a thermal resistance that hinders heat propagation resulting in a discontinuity in surface temperature. By modeling the heat propagation, the surface temperature can be calculated when the surface is illuminated with a focused laser beam moving in a straight line. Fig. 22 shows the temperature profiles along the x axis for an AISI-304 sample with an infinite vertical crack at plane $x = 0$ [17].

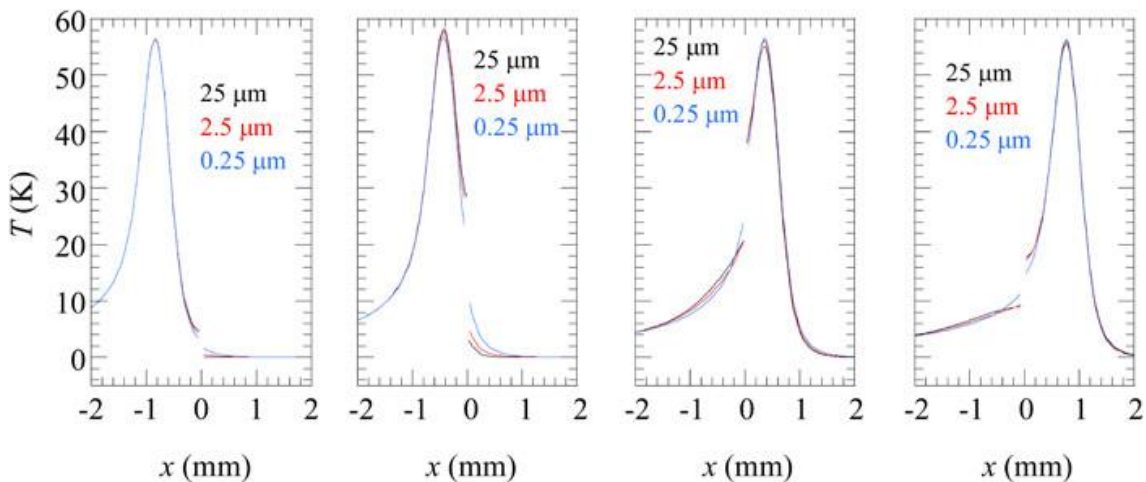


Figure 22 Sequence of temperature profiles along the x axis for an AISI-304 sample with an infinite vertical crack at plane $x = 0$

The idea is to determine what is the most relevant information (selected from the whole movie) and fit that experimental data to the already calculated theoretical expression to obtain the crack width and penetration.

It's worth mentioning that the jump the discontinuity of the surface temperature presents is dependent on the distance between the laser spot and the crack. The closer the laser spot is to the crack the larger the discontinuity is.

References

- [1] "wikipedia," [Online]. Available: https://en.wikipedia.org/wiki/Thermal_diffusivity. [Accessed 04 09 2022].
- [2] C. Ibarra-Castanedo, J. R. Tarpani and X. P V Maldague, "Nondestructive testing with thermography," *European Journal of Physics*, p. S91, 2013.
- [3] C. Ibarra-Castanedo, J. R. Tarpani and X. P V Maldague, "Nondestructive testing with thermography," *European Journal of Physics*, pp. S92-S96, 2013.
- [4] B. Zhang and R. Imhof, "Theoretical analysis of the surface thermal wave technique for measuring the thermal diffusivity of thin slabs," *Appl. Phys. A-Mater. Sci. Process.* 64 (2), p. 323, 1996.
- [5] N. W. Pech-May, A. Mendioroz and A. Salazar, "Simultaneous measurement of the in-plane and in-depth thermal diffusivity of solids using pulsed infrared thermography with focused illumination," *NDT&E International* 77, p. 28, 2016.
- [6] A. Salazar, M. Colom and A. Mendioroz, "Laser-spot step-heating thermography to measure the thermal diffusivity of solids," *Int. J. Thermal Sci.* 170, p. 107124, 2021.
- [7] Y. Wang, P. Kuo, L. Favro and R. Thomas, "A novel "flying-spot" infrared camera for," *Photoacoustic and photothermal phenomena. II Springer series in optical sciences*, 62, p. 24, 1990.
- [8] C. Gruss and D. Balageas, "Theoretical and experimental applications of the flying spot camera," QIRT Conference, Paris, 1992.
- [9] I. Gaverina, M. Bensalem, A. Bedoya, J. González, A. Sommier, J. Battaglia, A. Salazar, A. Mendioroz, A. Oleaga, J. Batsale and C. Pradere, "Constant Velocity Flying Spot for the estimation of in-plane thermal diffusivity on anisotropic materials," *International Journal of Thermal Sciences*, vol. 145, p. 1, 2019.
- [10] A. Salazar, A. Mendioroz and A. Oleaga, "Flying spot thermography: Quantitative assessment of thermal diffusivity and crack width," *Journal of Applied Physics*, pp. 5-7, 2020.
- [11] A. Salazar, A. Mendioroz and A. Oleaga, "Flying spot thermography: Quantitative assessment of thermal diffusivity and crack width," *Journal of Applied Physics*, p. 6, 2020.
- [12] A. Salazar, A. Mendioroz and A. Oleaga, "Flying spot thermography: Quantitative assessment of thermal diffusivity and crack width," *Journal of Applied Physics*, p. 7, 2020.
- [13] "Silloptics," [Online]. Available: <https://www.silloptics.de/en/service/sill-technical-guide/laser-optics/f-theta-lenses#:~:text=The%20use%20of%20C6%92%2Dtheta,proportional%20to%20the%20scan%20angle..> [Accessed 12 09 2022].
- [14] "Thorlabs," [Online]. Available:

https://www.thorlabs.com/newgrouppage9.cfm?objectgroup_id=10766. [Accessed 12 09 2022].

- [15] Y. Çengel, Heat Transfer: a Practical Approach, Boston: McGraw-Hill, 2033.
- [16] "Goodfellow catalogue," [Online]. Available: <http://www.goodfellow.com>.
- [17] A. Salazar, A. Mendioroz and A. Oleaga, "Flying spot thermography: Quantitative assessment of thermal diffusivity and crack width," *Journal of Applied Physics*, p. 9, 2020.

Appendix I

FLYING SPOT SOFTWARE

Interface

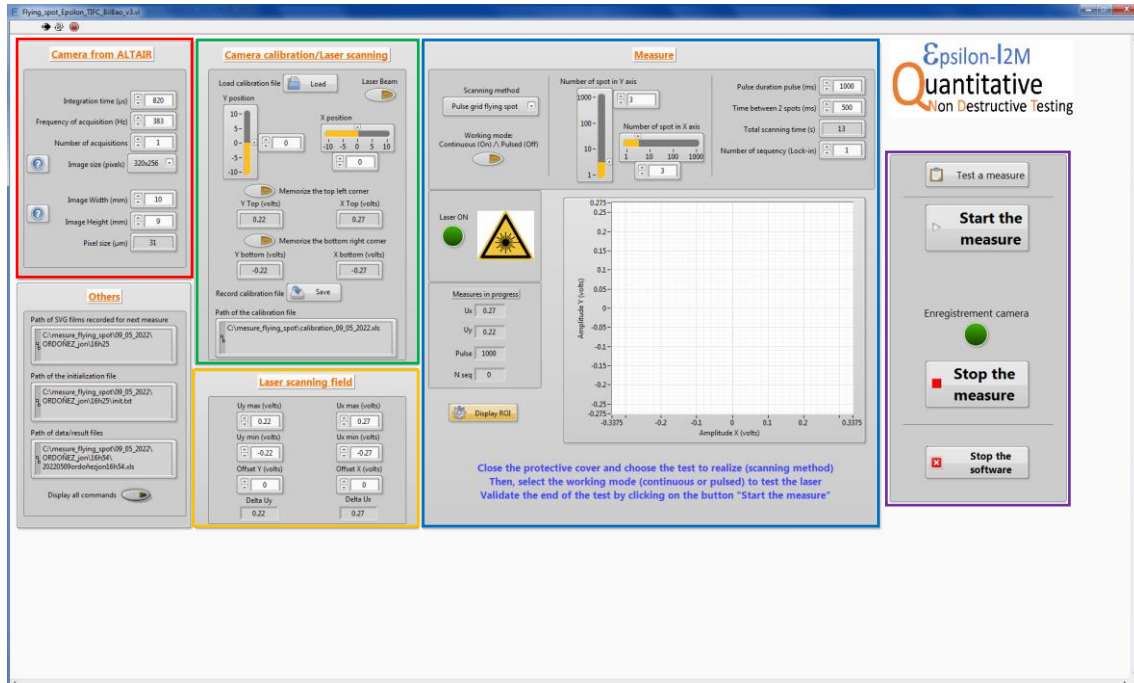


Figure 23 Flying spot software interface

This is the basic interface of the flying spot software. When the program is first opened a window will pop up where the user needs to put their name, last name, the number of the measurement there are going to do, and the name of the material being analyzed. Once that information is introduced, this is the interface that will appear.

As shown in the picture each section of the interface is marked except one, which is unimportant. This one only shows information about the measurement.

The user must keep in mind that BEFORE opening this software, Altair must already be opened and with the live camera feed ON.

Camera from ALTAIR

In this **Camera from ALTAIR** section is where the user must input the parameters previously selected in Altair's Camera tab. The integration time, frame rate and the size of the image in millimeters. This is done by introducing the width and the height. This is calculated by multiplying the length of each pixel by the number of pixels in each direction. In this case the size of each of the camera's pixels is $30\ \mu\text{m}$. So, the image width would be 30×320 , 9.6mm. The height would be 30×256 , 7.68mm. The software only admits integer numbers, so when the user inputs those numbers, the software will change them to 10 and 8 respectively. Resulting in a pixel size displayed as 31. The user may be tempted to input 10 and 8 directly, but his may result in a pixel size greater than 31 due to a possible glitch, so the best bet is to input the real values and let the software correct them.

Camera calibration/Laser scanning

In this **Camera calibration/Laser scanning** section, the user will input the range of the camera by writing down the values of the voltage necessary to move the spot to the top left and bottom right corner of the camera.

With the Laser Beam button ON, the user must adjust the Y position and X position (enter the numbers and press intro). Back in Altair, on the live feed, the user will see the spot has changed positions each time those values change. The user must keep adjusting this position until the spot is in the top left corner of the live camera. Once the spot is there, press 'Memorize the top left corner'. The exact same process must be done to move the laser to the bottom right corner of the live camera. Then, the user must press 'Memorize the bottom right corner'. Once both corners have been memorized, hit 'Save'. A calibration file (.xls) will be generated at a set location. The user can 'Load' this file at later times in order to avoid having to calibrate the camera again.

Laser scanning field

In this **Laser scanning field** section, the user determines the limits of the field the spot will be moving in. This field can be larger or smaller than the camera field previously calibrated. The camera field won't change because the camera is always the same. However, this scanning field may change from one measurement to another. If the user chooses for these limits to be the physical corners of the sample (typically larger than the camera field), when changing samples, if the size of those change, this limit values must also be changed. The user must select this by moving the laser like in the previous section, only this time, the user must look at the sample, not the live camera, because the spot will be outside the camera field. The software doesn't give the option to save these values in any way, so if more than one measurement is going to be done with the same sample, the user must right down or memorize these values and input them each time a measurement is going to be done.

Measure

In this **Measure** section, the user will determine various parameters of the measurement.

Working mode: Continuous (On)/Pulsed (Off)

The main difference between these modes is that the shutter stays open in continuous mode and it opens and closes in pulsed mode. The other important difference is how the duration work. This is best explained with an example.

Let it be:

Pulse duration: 1000 ms (time the shutter will stay opened in pulsed mode)

Time between 2 spots: 1000 ms (time the shutter will remain closed in pulsed mode before opening again)

Number of sequency: 2 (number of times the open-closing sequence will happen in each spot)

With this configuration, in pulsed mode, the following will happen, all on the same spot. Opened 1 second, closed 1 second, opened 1 second and closed 1 second, end of the measurement. A total of 4 seconds. In continuous mode, the shutter will be opened for all those 4 seconds. Since the shutter doesn't close, in continuous mode, if the user were to put 3 seconds of pulsed duration, 1 second of time between spots and 1 sequence, the result would be the exact same. The spot would be 4 seconds on each spot.

It's also important to note that the 'Total scanning time' displayed in each mode is different. This has also to do with the number of spots. So, the exact formula of this displayed time will be provided later on.

Scanning method: Pulse grid flying spot

Enter the number of spots in each axis. For instance, the resulting grid of entering Y:3 X:5 is:

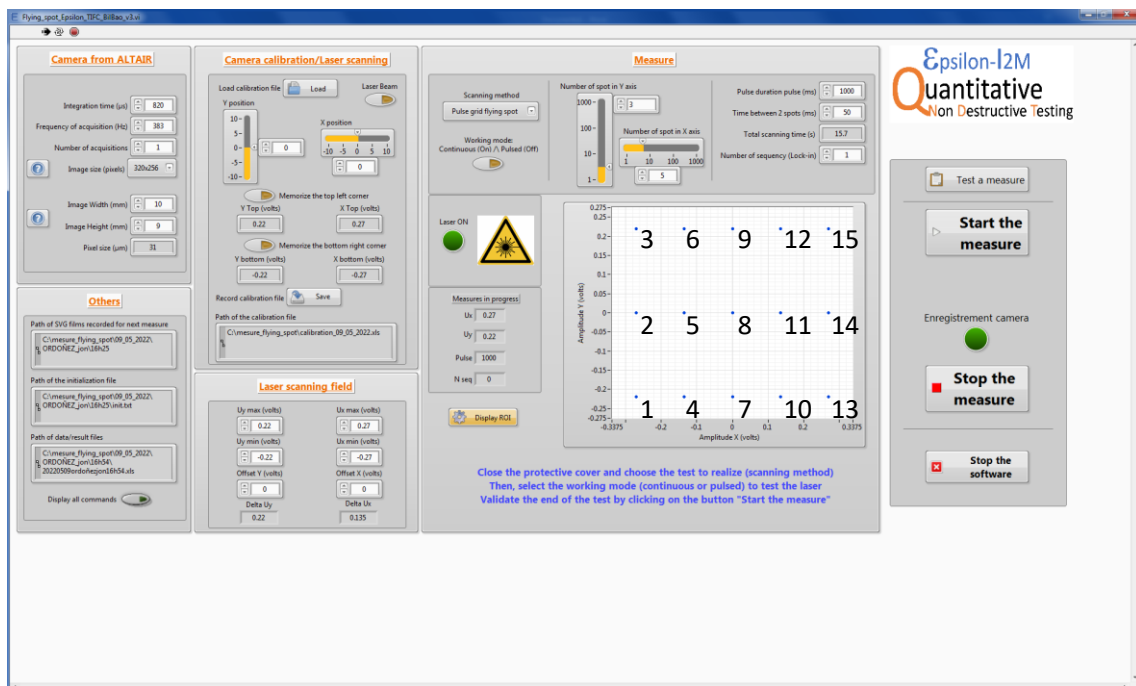


Figure 24 Pulse grid flying spot example

This grid is generated in the order written in the picture.

Working mode: Vertical line

Enter the number of spots in each axis. For instance, the resulting grid of entering Y:3 X:5 is:

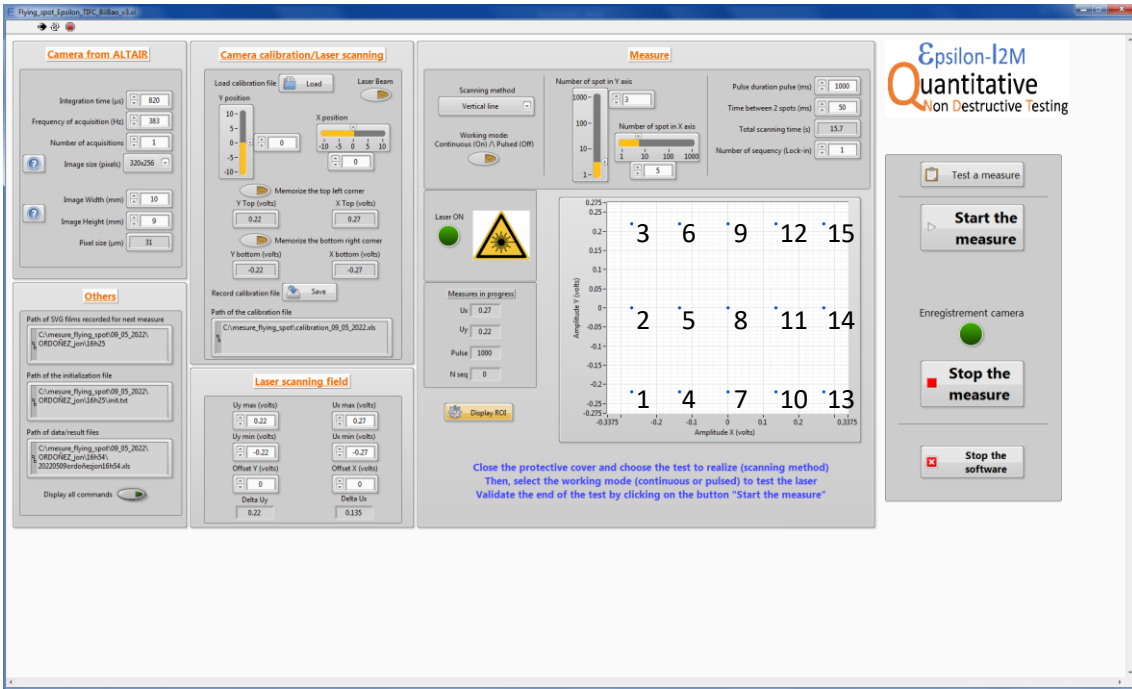


Figure 25 Vertical line example

The result is the exact same as in the pulse grid mode, in the exact same order.

Working mode: Horizontal line

Enter the number of spots in each axis. For instance, the resulting grind of entering Y:3 X:5 is:

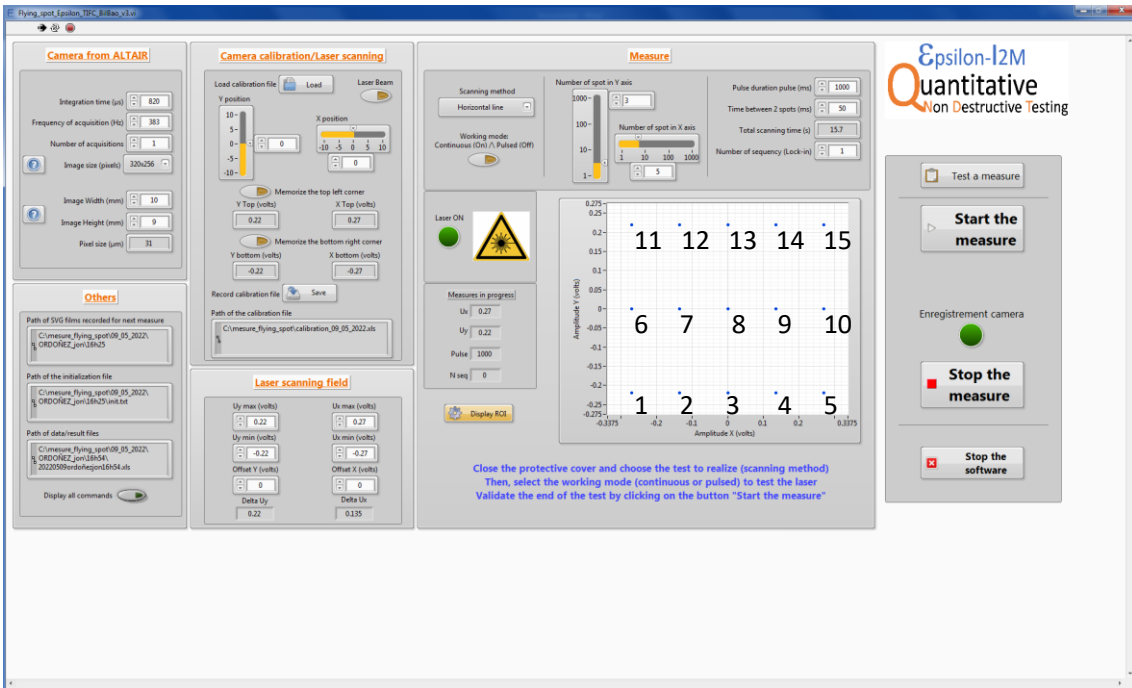


Figure 26 Horizontal line example

The resulting grid is the same as in the prior cases but done in a different order.

Working mode: Single line angle

Here the user enters the shoot angle and the number of points. The following resulting patterns were done at 45°, -45°, 90°, -90 degrees and 5 points.

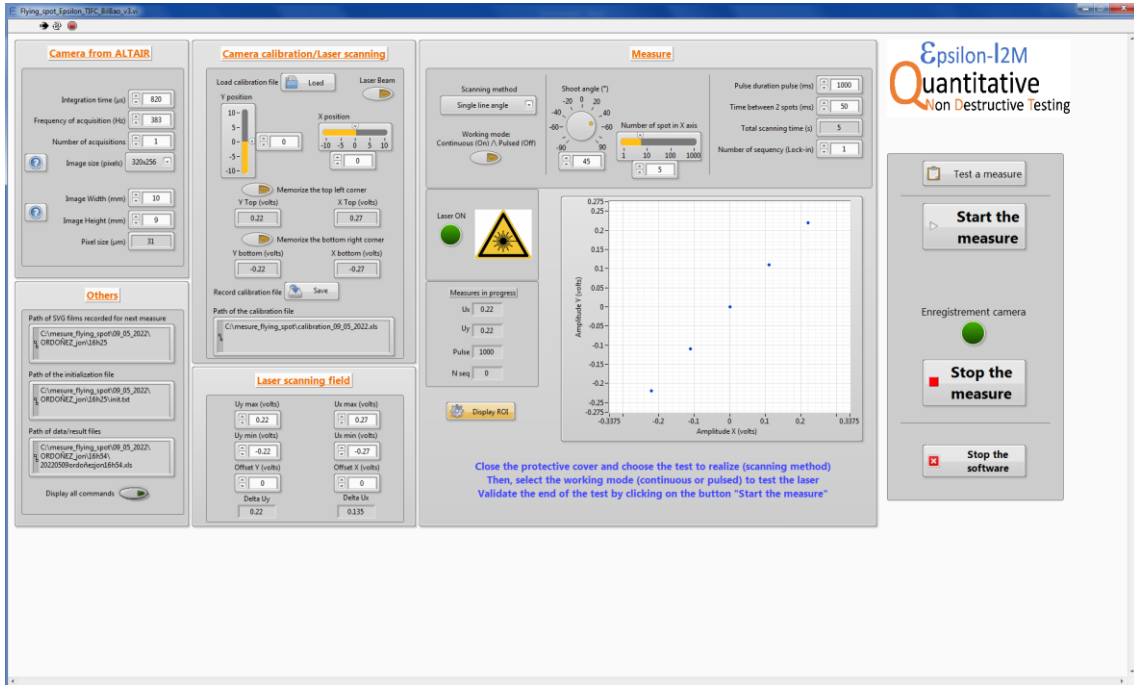


Figure 27 Single line angle at 45° example

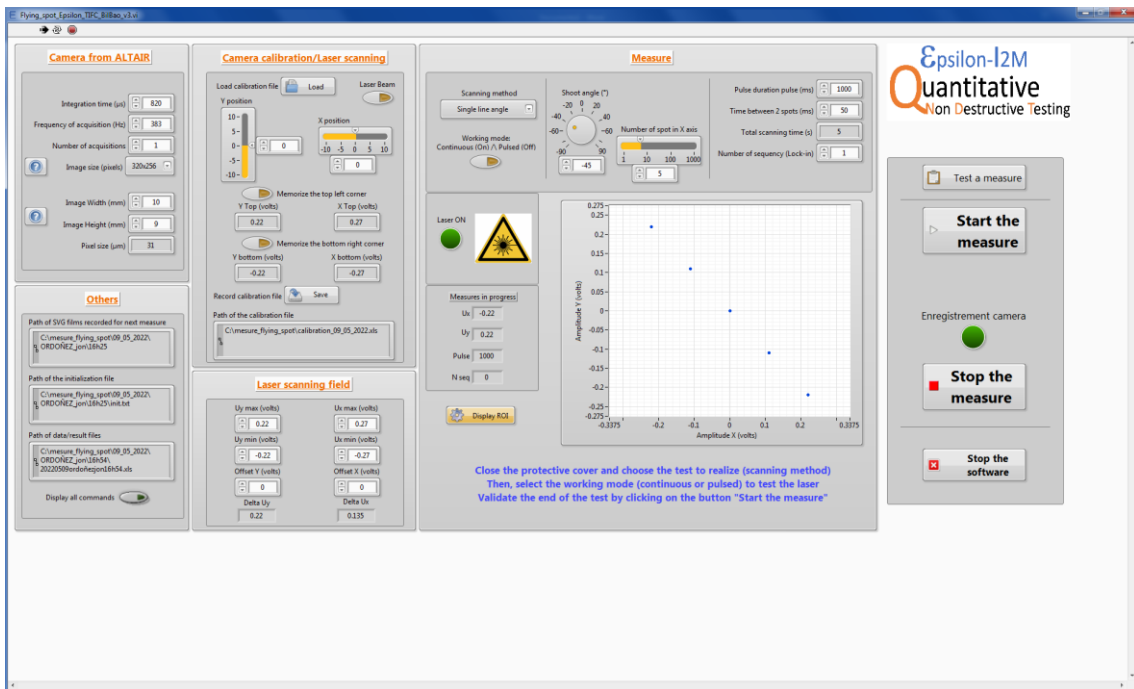


Figure 28 Single line angle at -45° example

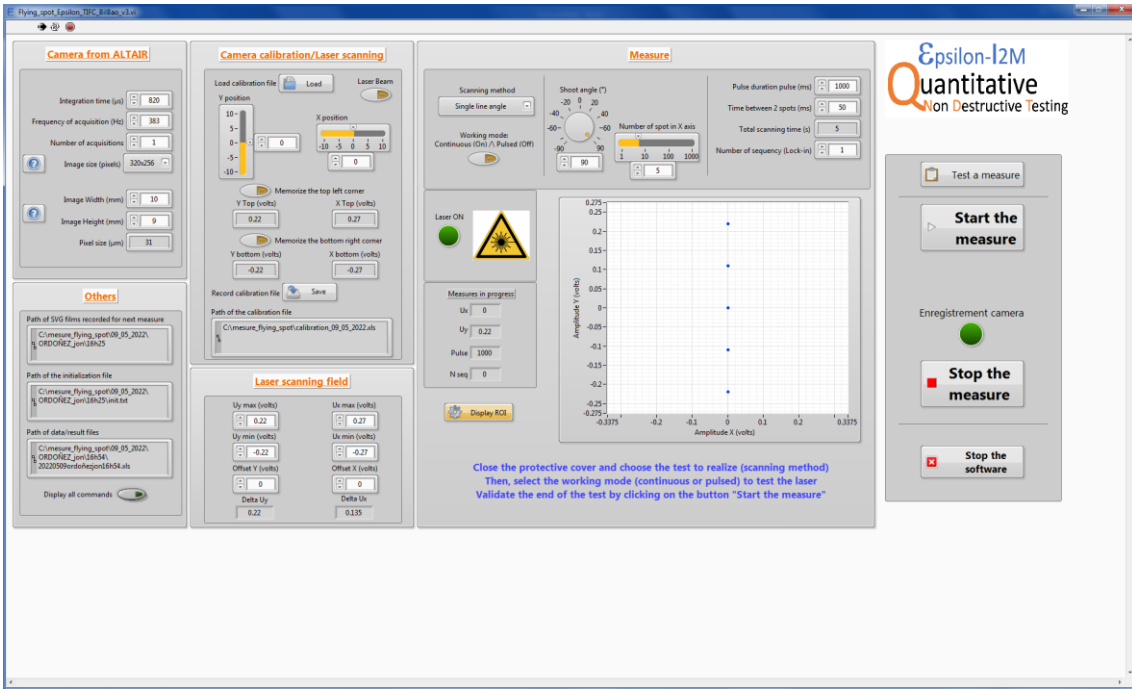


Figure 29 Single line angle at 90° example

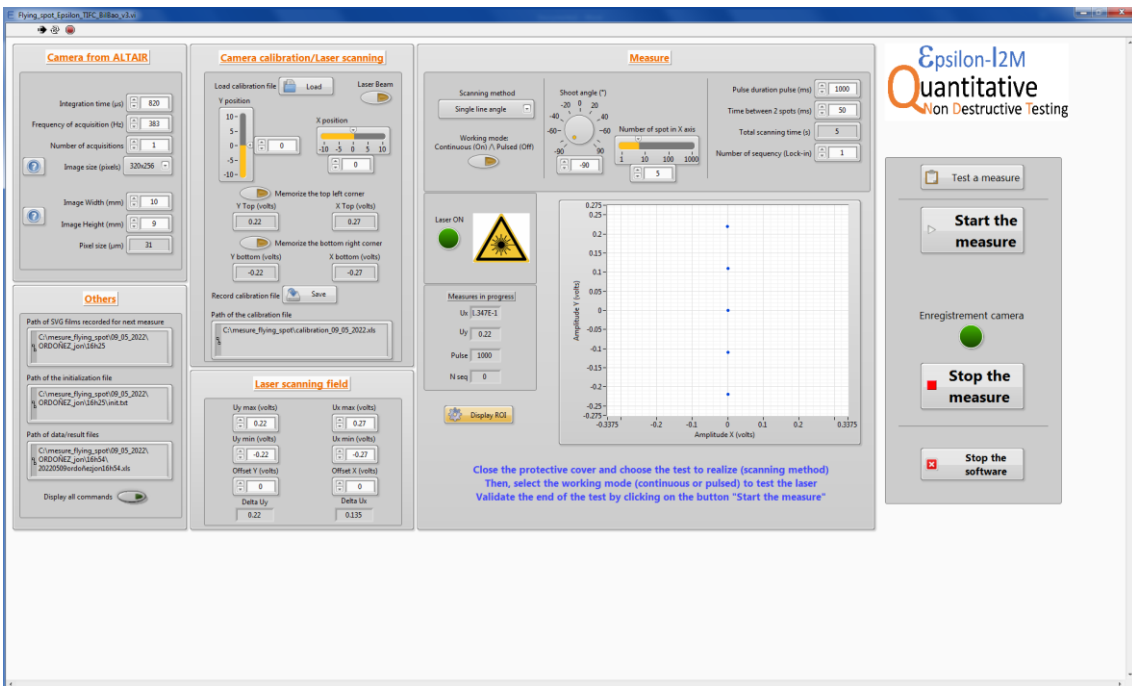


Figure 30 Single line angle at -90° example

All these grids are generated from bottom to top.

Positions of the spots

The software calculates the distance and placements of each point based on the range (max, min of the cartesian directions) of the laser scanning field, (0,0) being the symmetry point. So if we the user enters (1,1) (1 point in the X axis and 1 in the Y axis), it'll place single point at coordinates (0,0). If the user enters (3,1), it'll place one at

(min,0), one at (0,0) and another at (max,0). if the user enters (3,2), it'll place a point in (min,min), (0,min), (max,min), (min,max), (0,max) and (max,max). The software divides the range in equal portions for each direction, the symmetry point being at (0,0).

Displayed Total scanning time

In pulsed working mode it'll display a time equal to number of spots x (pulse duration + time between 2 spots) – 1 x time between 2 spots.

In continuous working mode the displayed time is number of spots x pulse duration.

In neither case the that displayed time matches the real duration of the measurement, so it's important to keep in mind and know how long the measure will take regardless of what this software says. This will be important when setting the duration of the movie.

Testing and Measuring

In this **Testing and Measuring** section, the user may test the measure with the selected parameter previously input like explained in the sections above. Once the user is satisfied with it, the 'Start the measure' button may be hit. Although more preparation is required as explained in the next section. Following those steps is vital for a successful measurement.

DETAILED PROCEDURE

1. Fill the Camera from Altair section up in the flying spot software, with the parameters from the camera.
2. In the Camera calibration/Laser scanning section, load the generated file, created as previously explained.
3. Enter the desired range in the Laser scanning field section.
4. Carefully enter the desired parameters in the Measure section. There is an important glitch here. If the user wants to work on pulsed mode, there's no problem. Enter the values and it'll function correctly. To work on continuous mode, the user must introduce the parameters in pulsed mode first. Once they are introduced and ready to go if working on pulsed working mode, change the mode to continuous. The values will change, and the user must enter them again, now in continuous. After extensive testing it can be concluded that this must be done in this manner when working in continuous mode, otherwise it doesn't work properly. First enter them in pulsed mode, then change to continuous and enter them again.
5. Click the 'Display ROI' button.

- Back in Altair, in the Recorder tab. Click on 'Advance...' and make sure the following is checked in the window that pops up and the click OK.

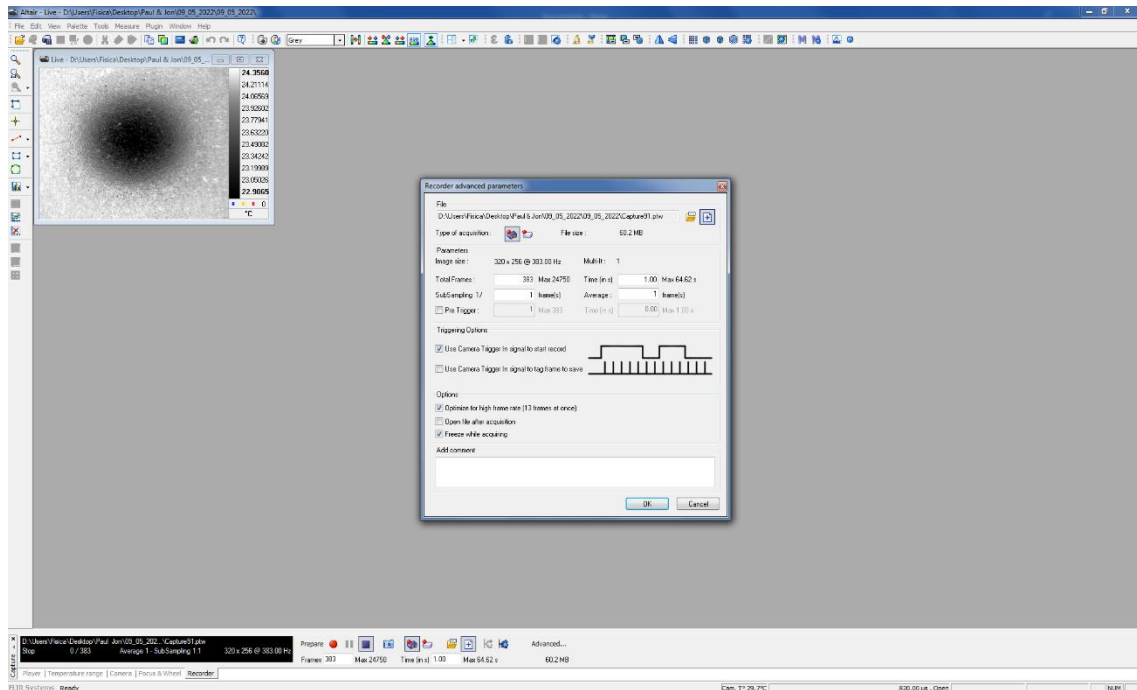


Figure 31 Measurement preparation 1

- Click the recorder trigger and the following window will pop up. Make sure only 'Single event' is checked. Then click OK. This will reset whatever recording time might be set to 1. This is why the user must select the time AFTER this step.

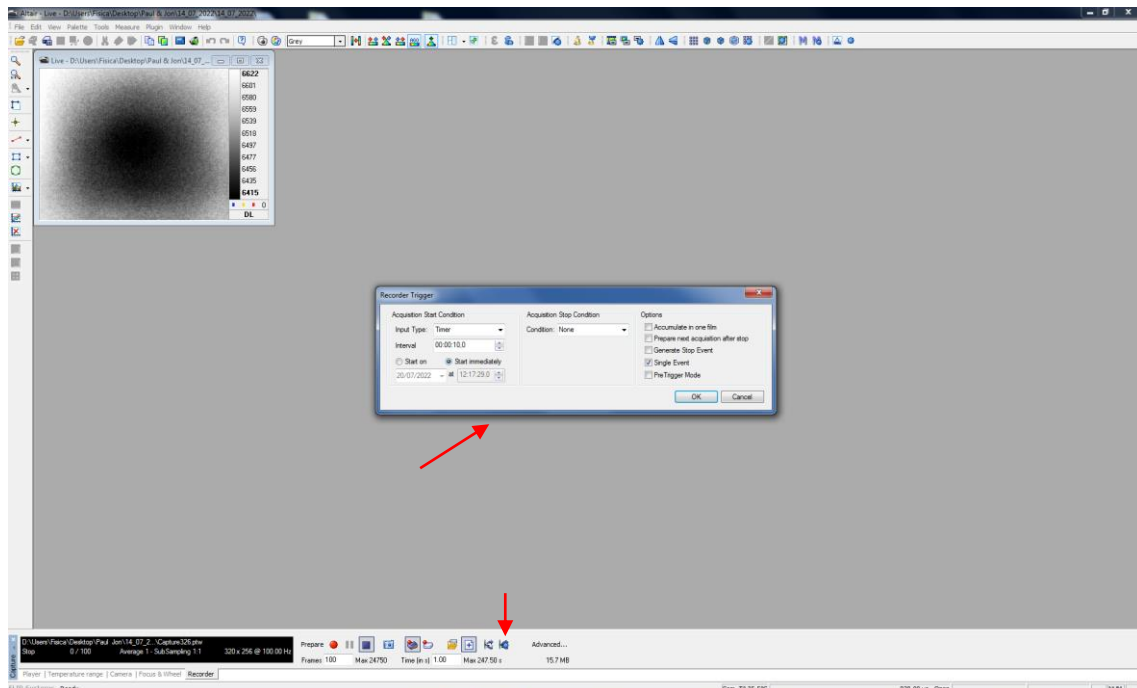


Figure 32 Measurement preparation 2

8. Now the user sets the time of the movie. This time **MUST** be lengthier than the duration of the measurement. There is a delay between the time the measurement starts and the time the recording starts. To avoid any problems, the length of the movie must be **AT LEAST 2 seconds** longer than the duration of the measurement. Therefore, knowing how durations work with both working modes is important, and knowing the displayed time is not to be completely trusted, as explained in previous sections. So, the user must know how long the measurement will take and add 2

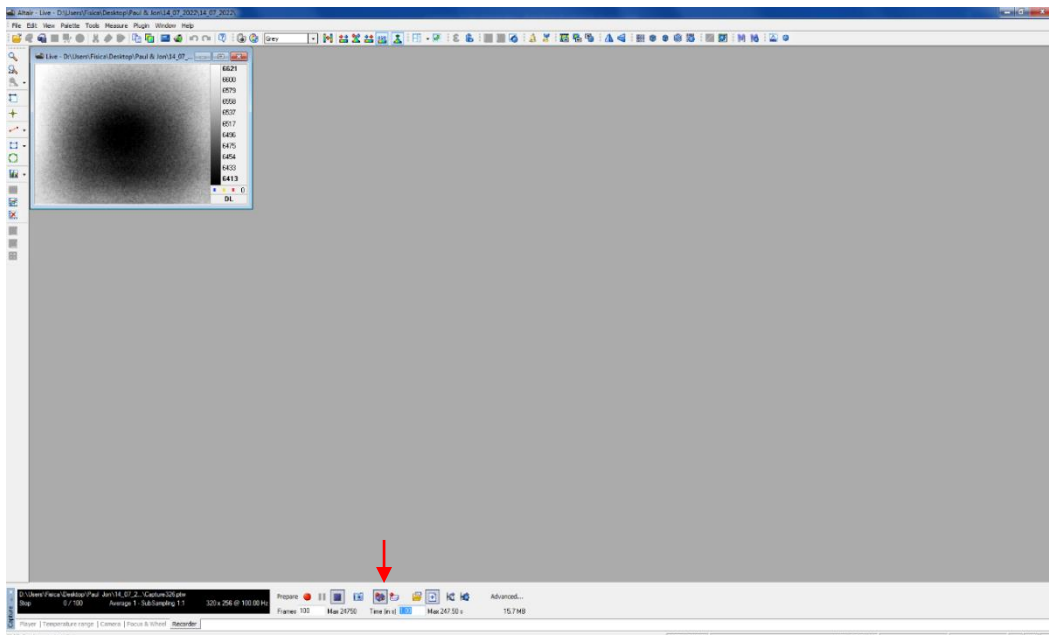


Figure 33 Measurement preparation 3

seconds to that. This is the time that will be input here and press intro to confirm.

9. The following figure shows how the interface should look like after clicking on the recording trigger (the marked icon), it stays checked. Now everything is in place and ready to go.

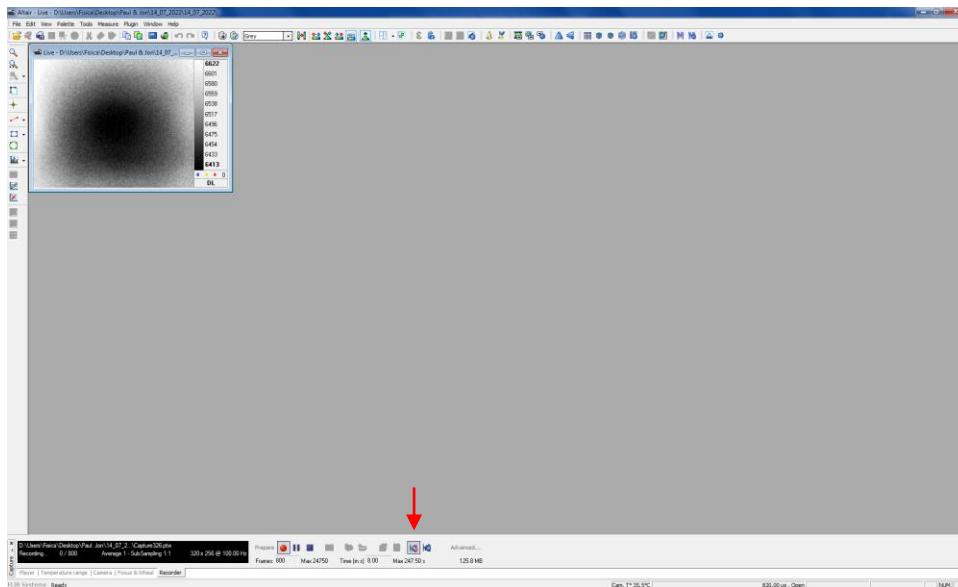


Figure 34 Measurement preparation 4

10. Now, back at the flying spot software, hit the ‘Start the measure’ button and the measurement and the recording will begin. When it finishes, a movie will be saved. This movie can be opened in ALTAIR, so the user may analyze it.

11. To do another measurement, the user must uncheck the recording trigger in ALTAIR. In the flying spot software, in the top left corner of the interface there will be a white arrow. The user must click it and re-enter their name, last name, number of measurement and material name. The parameters of the camera won’t be gone, so no need to enter them again. Same goes for the Laser scanning field, though it can be changed if the user switches samples. The only thing the user must do is load the calibration file again and enter the measurement parameters over the Measure section. Now repeat steps 6-10.

Appendix II

```
clear
clc
% convert PTW to Matlab file. Kelly M
fr=700; %frame total
imax=256; % rows per frame

for i=0:fr-1;
    GetPTWFrame('Capture319.pts',i+1);
    frame{i+1}=data(1:imax,:);
    frame=frame;
end
save('Capture319','frame');
filas=length(frame{1}(:,1));
col=length(frame{1}(1,:));
pixels=filas*col;
frames=length(frame);
```

Appendix III

```
% Laser spot velocity calculator used after PTWtoMatlab.m
for i=1:length(frame)
    m=cell2mat(frame(1,i));
    v=mean(m,1);
    a(i,:)=v;
end
a;
a_t=a';
[M,N] = size(a_t);
[xx, yy]=meshgrid(1:N,1:M);
fps=100; % enter the frames per second of the movie
pcolor(xx/fps,0.03*yy,a_t); % 0.03 is multiplied to convert to mm
figure

minfr=178; % enter number of the first frame in which the spot
appears in the FOV
maxfr=358; % enter number of the last frame in which the spot
appears in the FOV
[Y,I]=max(a_t(:, [minfr:maxfr]));
l=length(I);
xx=(1:l)/fps;
yy=I*0.03;
b0=ones(length(xx), 1);
XX=[b0 xx'];
YY=yy';
rl=XX\YY; % this is the value of the velocity in mm/s
RL=XX*rl;
plot(xx,yy, '.');
hold on
plot(xx,RL);
grid on
```

Appendix IV

```
%Longitudinal profiles

n=(306-294); % enter the interval of frames to be averaged

% extraction of the longitudinal profiles

for i=0:n-1
    pl=cell2mat(frame(1,294+i)); % enter the first frame
    perfiles(1,i+1)=mat2cell(pl);

end

for i=0:n-1
    pl=cell2mat(perfiles(1,i+1));
    lo=pl(141,:); % 141 is number of th epixel representing the
height of the laser spot
    Longi(i+1,:)=lo;
end

[M N]=size(Longi);
[Y I]=max(Longi, [], 2);
for i=1:M
    d=[1:N];
    Longidist(i,:)=d-I(i); % contains x-axis of each profile, with
the origin located at the maximum in each case
end

% the following lines sort the profiles in such a way that they
disregard the x-axis points

% not contained in the last frame's profile by assigning tho these
points an absurd value like 1000

c=Longidist(M,1);
for i=1:M
    v=Longidist(i,:);
    f=find(v==c);
    for k=1:f-1
```

```

        v(k)=1000;
    end
    Longidist2(i,:)=v;
end
Longidist3=sort(Longidist2,2);
Longi2=ones(M,N)*1000;
for i=1:M
    w=Longidist2(i,:);
    indx_nonthousand=find(w < 1000);
    indx_thousand=find(w > 999);
    u=Longidist2(i,indx_thousand);
    w=Longi(i,indx_nonthousand);
    Longi2(i,:)=[w u];
end

% plotting and avarage calculation of ln(|Tx|)

for i=1:N
    x=Longidist3(:,i)*0.03;
    T=Longi2(:,i);
    indx_nonthousand_x=find(x < 1000);
    indx_nonthousand_T=find(T < 1000);
    x=x(indx_nonthousand_x);
    T=T(indx_nonthousand_T);
    t=length(T);
    ln_Tx_k=ones(t,1)*10;
    Tx=ones(t,1)*10;
    for k=1:t % for each element of column i
        Tx(k)=T(k)*x(k);
        ln_Tx_k(k)=log(abs(Tx(k))); % ln(Tx) is calculated, element
by element
    end
    ln_Tx(i)=mean(ln_Tx_k);
end
Longidist3r=Longidist3(M,1:length(Longi2))'*0.03;
plot(Longidist3r,ln_Tx,'o');

```

Appendix V

```
%Transverse profiles

n=(358-178) % enter the interval of frames to be averaged

% extraction of the longitudinal profiles

for i=0:n-1
    pt=cell2mat(frame(1,178+i)); % enter the first frame
    perfiles(1,i+1)=mat2cell(pt);

end

for i=0:n-1
    pt=cell2mat(perfiles(1,i+1));
    vec=pt(141,:); % 141 is number of th epixel representing the
height of the laser spot
    [Y,I] = max(vec);
    tr=pt(:,I);
    Transv(:,i+1)=tr;
end

[M N]=size(Transv);
[Y I]=max(Transv, [], 1);
for i=1:N
    d=[1:M]';
    Transvdist(:,i)=d-I(i)';
end

% plotting and avarage calculation of ln(|Ty|)

Transvdistr=Transvdist*0.03;
for i=1:N
    y=Transvdistr(:,i);
    T=Transv(:,i);
    for k=1:M % for each element of column i
        Ty(k)=T(k)*y(k);
```



```
        ln_Ty_k(k)=log(abs(Ty(k))); % ln(Ty) is calculated, element
by element
    end
    ln_Ty_i(:,i)=ln_Ty_k';
end
ln_Ty=mean(ln_Ty_i,2);
y=mean(Transvdistr,2);
plot(y,ln_Ty,'o');
hold off
```